

2-5-2002

Synthetic polyester absorbent materials

Bobby Mal Phillips

Shriram Bagrodia

Follow this and additional works at: https://tigerprints.clemson.edu/clemson_patents

Recommended Citation

Phillips, Bobby Mal and Bagrodia, Shriram, "Synthetic polyester absorbent materials" (2002). *Clemson Patents*. 149.
https://tigerprints.clemson.edu/clemson_patents/149

This Patent is brought to you for free and open access by TigerPrints. It has been accepted for inclusion in Clemson Patents by an authorized administrator of TigerPrints. For more information, please contact kokeefe@clemson.edu.



US006344595B1

(12) **United States Patent**
Phillips et al.

(10) **Patent No.: US 6,344,595 B1**
(45) **Date of Patent: Feb. 5, 2002**

- (54) **SYNTHETIC POLYESTER ABSORBENT MATERIALS**
- (75) Inventors: **Bobby Mal Phillips**, Jonesborough;
Shriram Bagrodia, Kingsport, both of
TN (US)
- (73) Assignee: **Clemson University Research
Foundation**, Clemson, SC (US)

5,140,076 A	8/1992	Hatsuda et al.	525/375
5,151,465 A	9/1992	Le-Khac	524/549
5,200,248 A	4/1993	Thompson et al.	428/131
5,242,644 A	9/1993	Thompson et al.	264/177.15
5,268,229 A	12/1993	Phillips et al.	428/400
5,611,981 A	3/1997	Phillips et al.	264/130
5,648,142 A	7/1997	Phillips	428/132
6,103,376 A	8/2000	Phillips et al.	428/397

FOREIGN PATENT DOCUMENTS

EP	0 450 923 A2	10/1991
WO	WO 89/10446	11/1989

(*) Notice: Subject to any disclaimer, the term of this patent is extended or adjusted under 35 U.S.C. 154(b) by 0 days.

* cited by examiner

Primary Examiner—Dennis Ruhl

(74) *Attorney, Agent, or Firm*—Kennedy Covington
Lobdell & Hickman, LLP

(21) Appl. No.: **09/303,859**

(22) Filed: **May 3, 1999**

Related U.S. Application Data

- (62) Division of application No. 08/916,071, filed on Aug. 21, 1997, now Pat. No. 5,977,429.
- (60) Provisional application No. 60/024,302, filed on Aug. 22, 1996.

- (51) **Int. Cl.**⁷ **A61F 13/15**
- (52) **U.S. Cl.** **604/370; 604/372**
- (58) **Field of Search** 604/358, 367,
604/370, 372, 378

References Cited

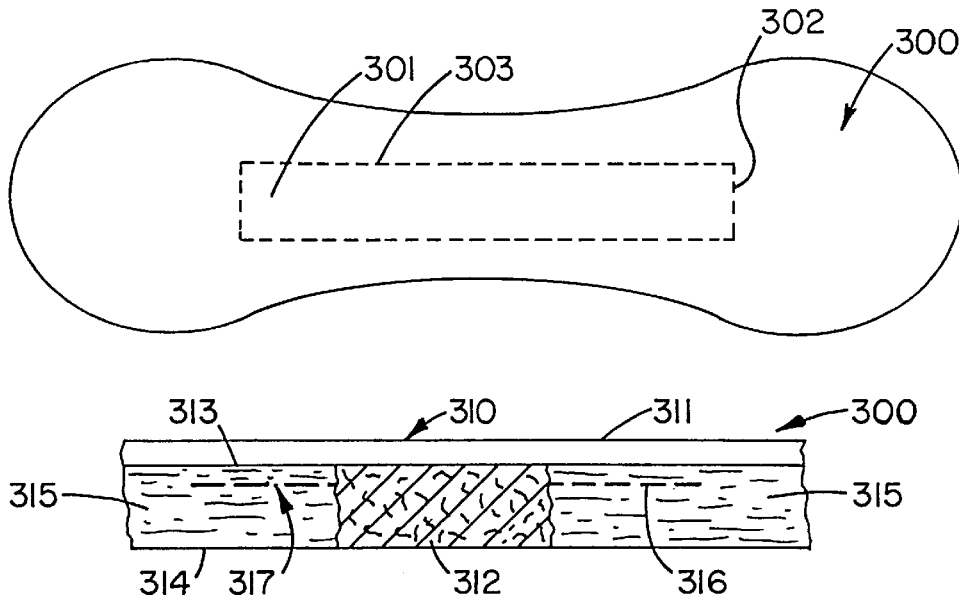
U.S. PATENT DOCUMENTS

3,219,739 A	11/1965	Breen et al.	264/177
4,223,677 A	9/1980	Anderson	128/287
4,888,093 A	12/1989	Dean et al.	162/157.6
4,889,596 A	12/1989	Schoggen et al.	162/157.6
4,898,642 A	2/1990	Moore et al.	162/157.6
4,976,819 A	12/1990	Minton	162/9
4,994,037 A	* 2/1991	Bernardin	604/378

(57) **ABSTRACT**

The invention provides synthetic polymeric fibers which have utility as temporary acquisition/distribution absorbent structures and permanent storage/distribution absorbent structures in a wide range of absorbent products such as diapers, feminine napkins, and adult incontinent pads. These fibers are short, highly distorted, and bulky characterized by lengths between 2 and 37 mm, short-range distortion factors between 5 and 70, long-range distortion factors between 0.05 and 0.9, and single fiber bulk factors between 0.5 and 10.0. They may or may not have capillary channels on the surface. The advantages of these materials are their increased absorbency, reduced wet collapse at low densities, reduced rewet, reduced loss of liquid under pressure, and their ability to be desorbed by distribution materials such as capillary channeled fibers or by conventional storage materials such as fluff pulp or superabsorbent polymer fiber or powder.

7 Claims, 32 Drawing Sheets



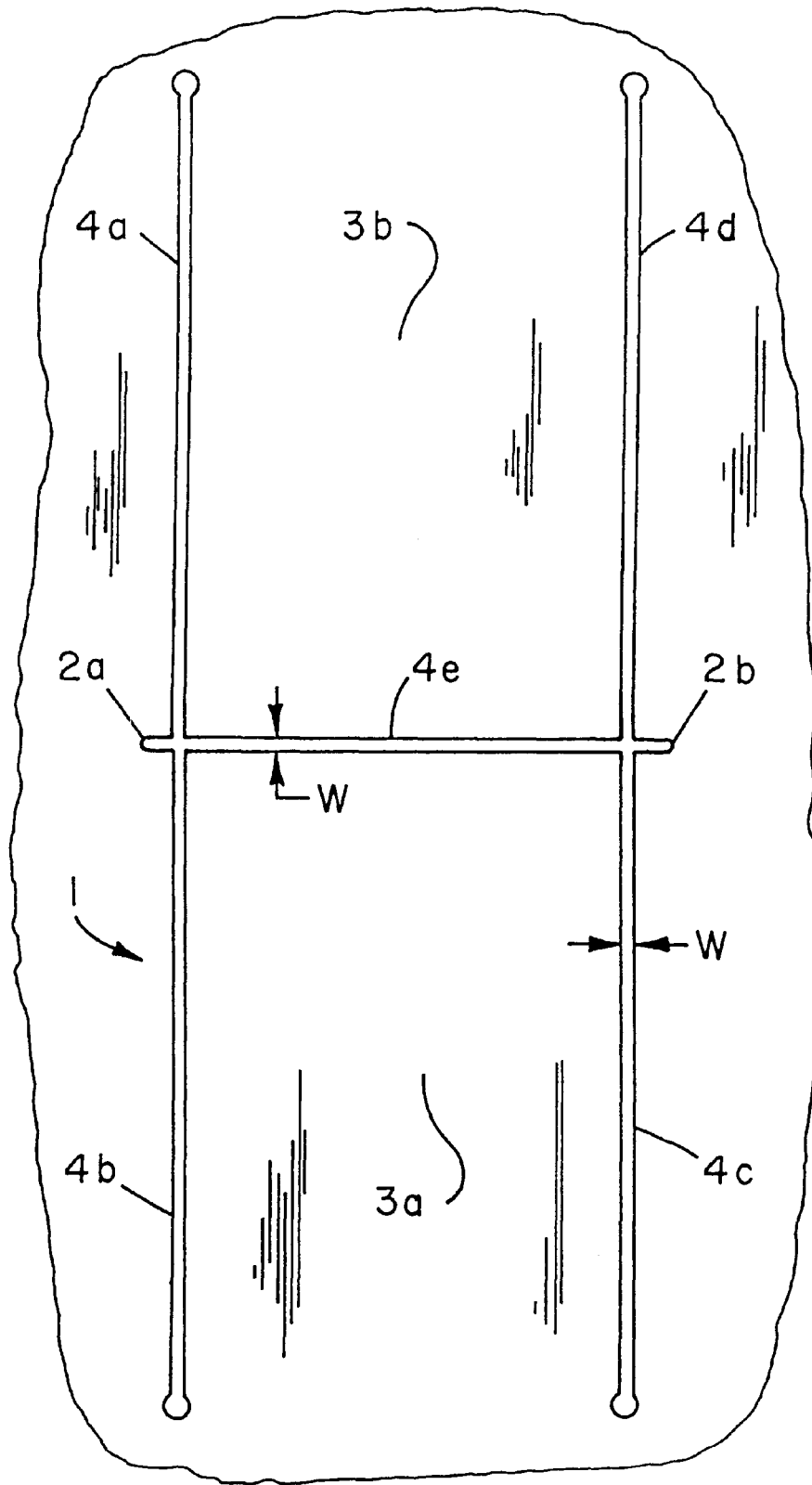


Fig. 1

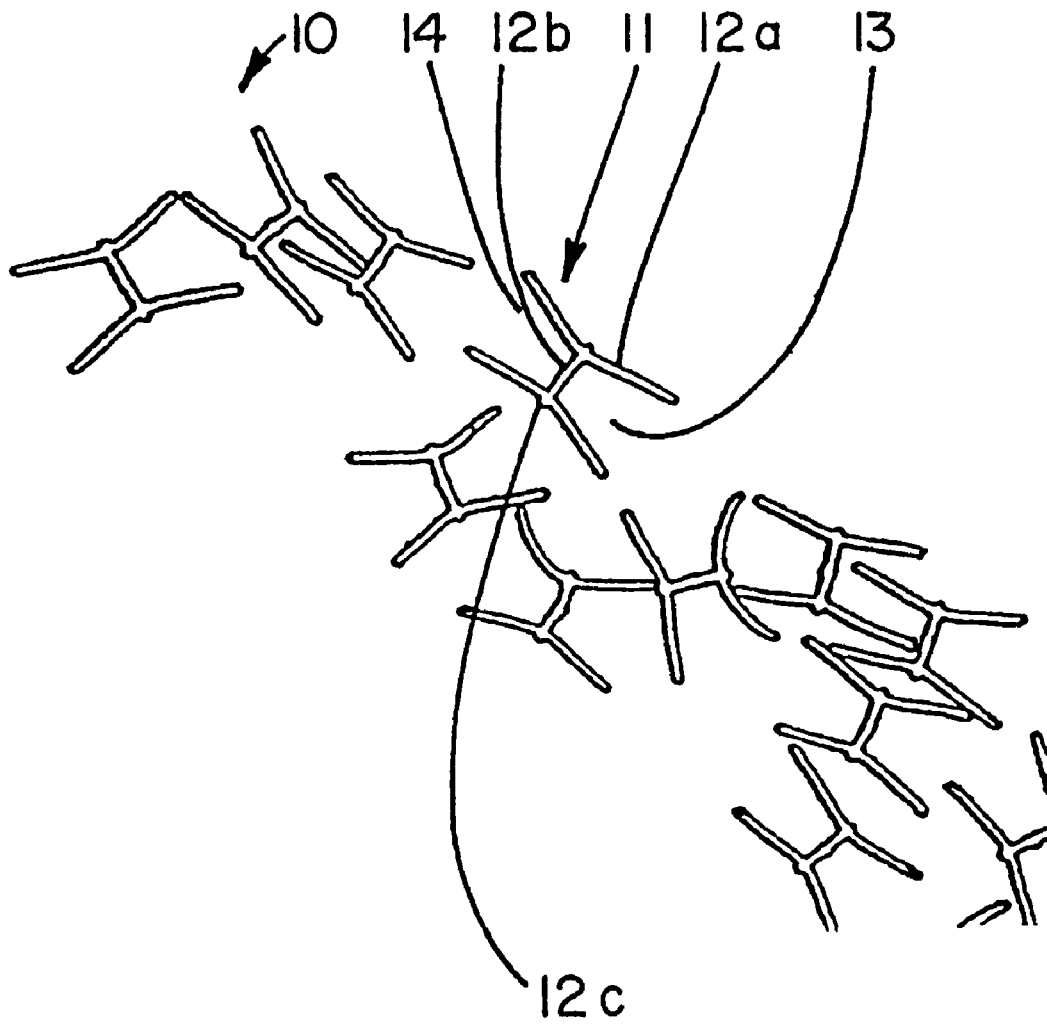


Fig. 2

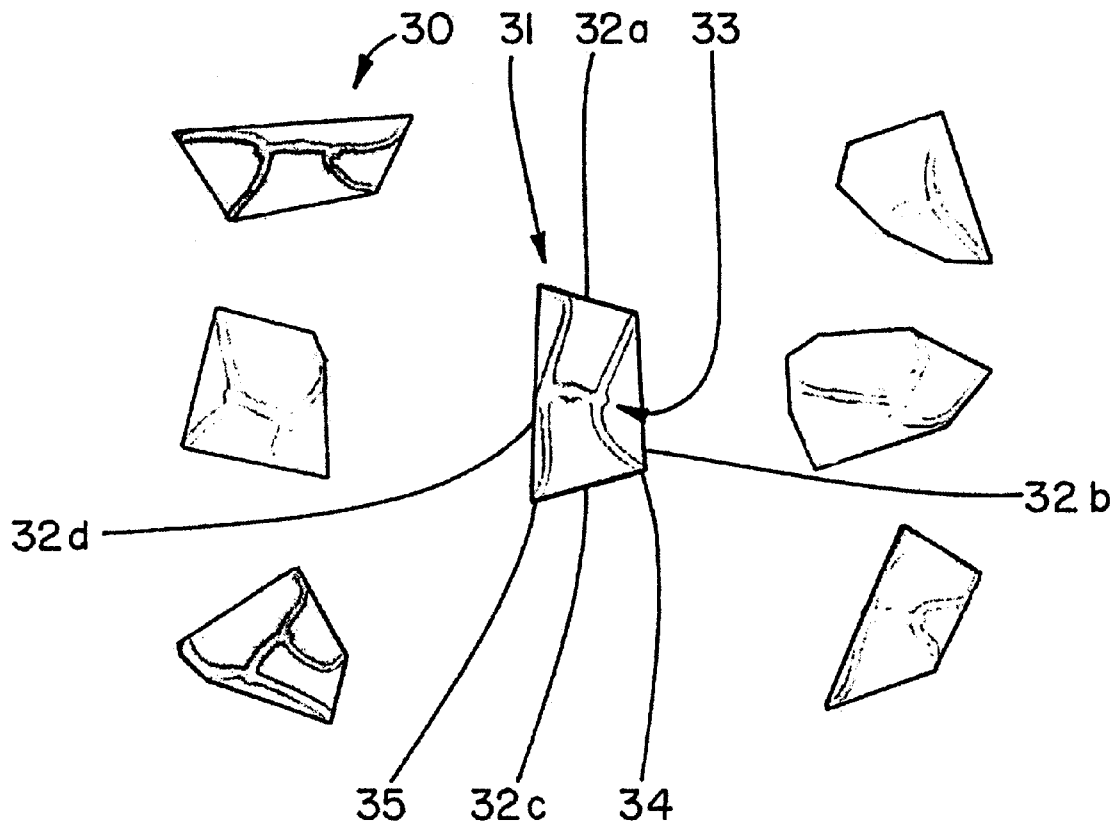


Fig. 3

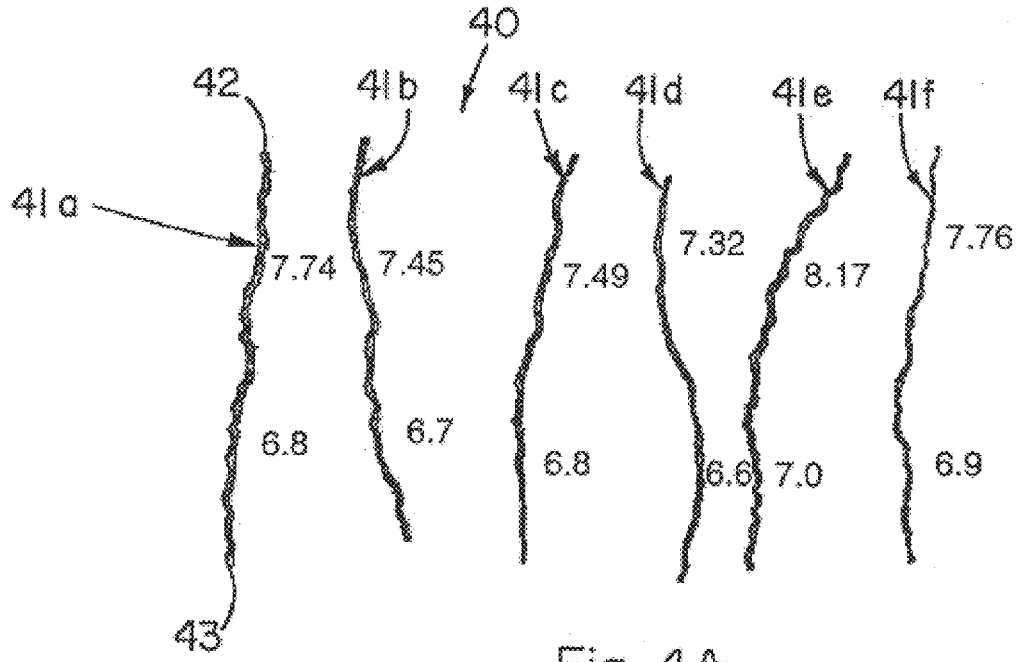


Fig. 4A

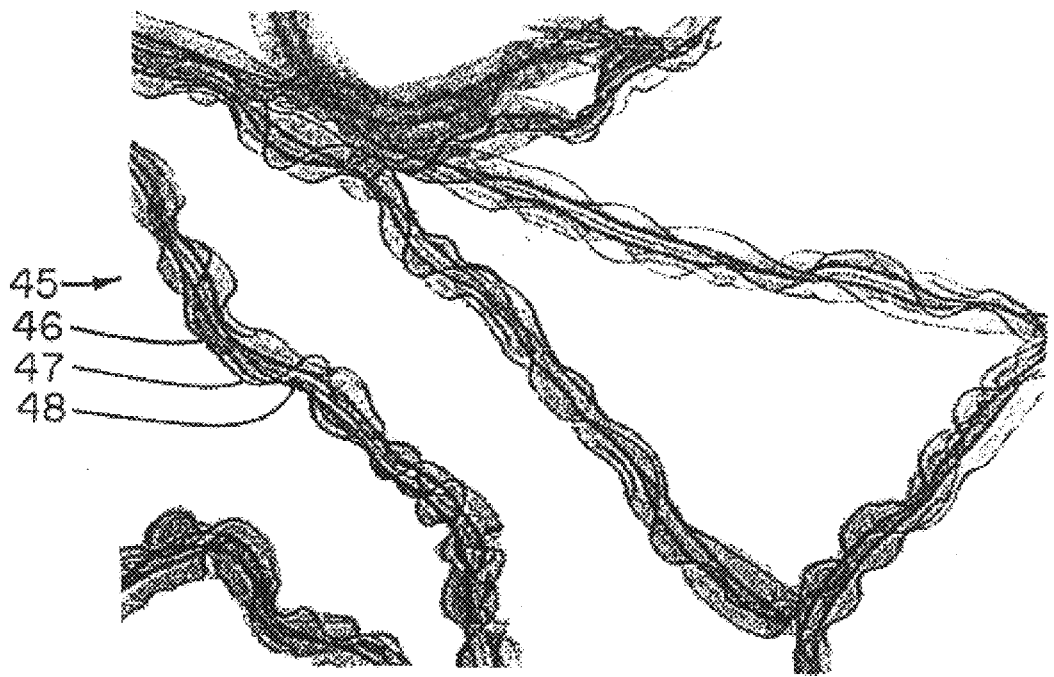


Fig. 4B

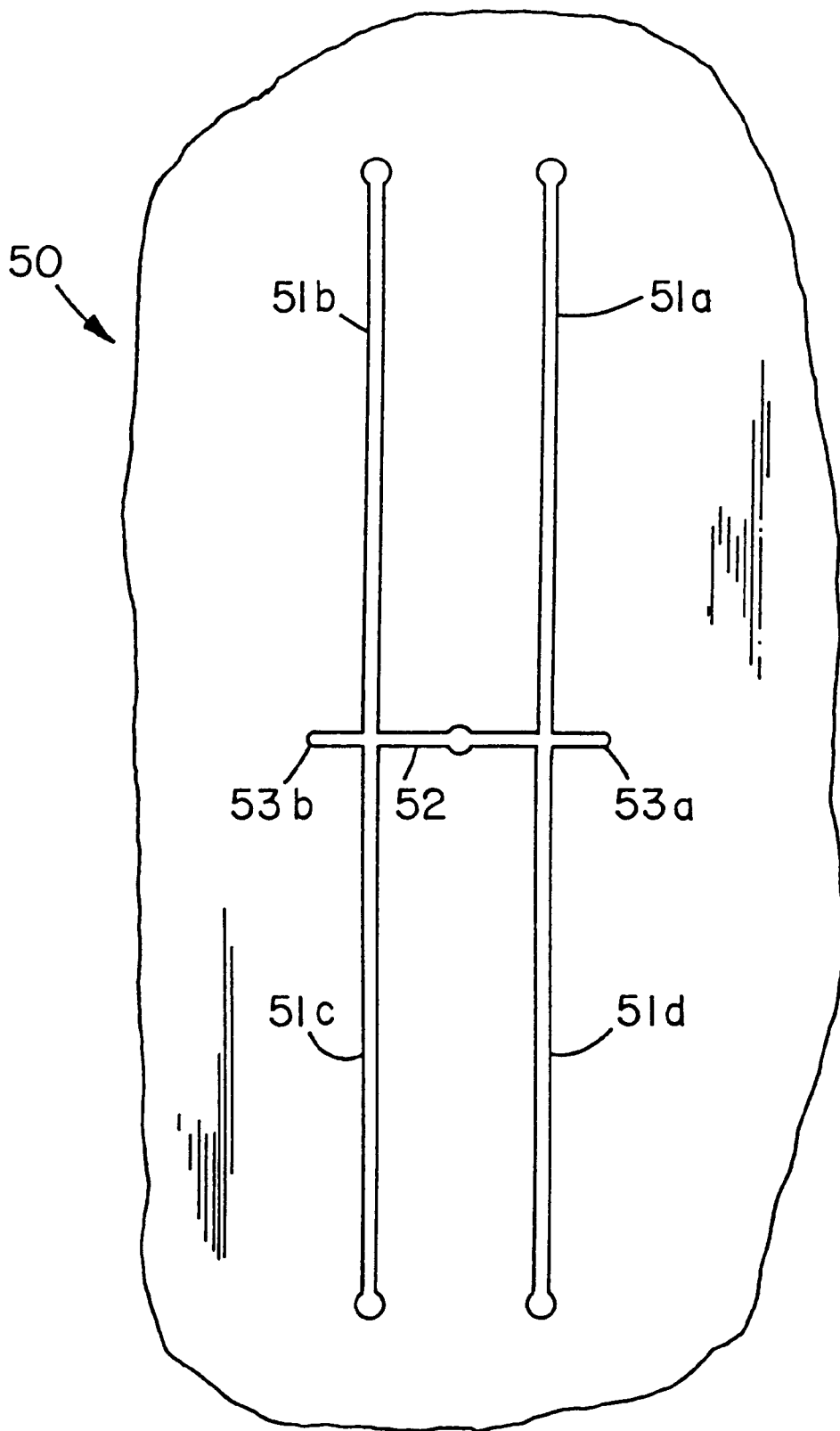


Fig. 5

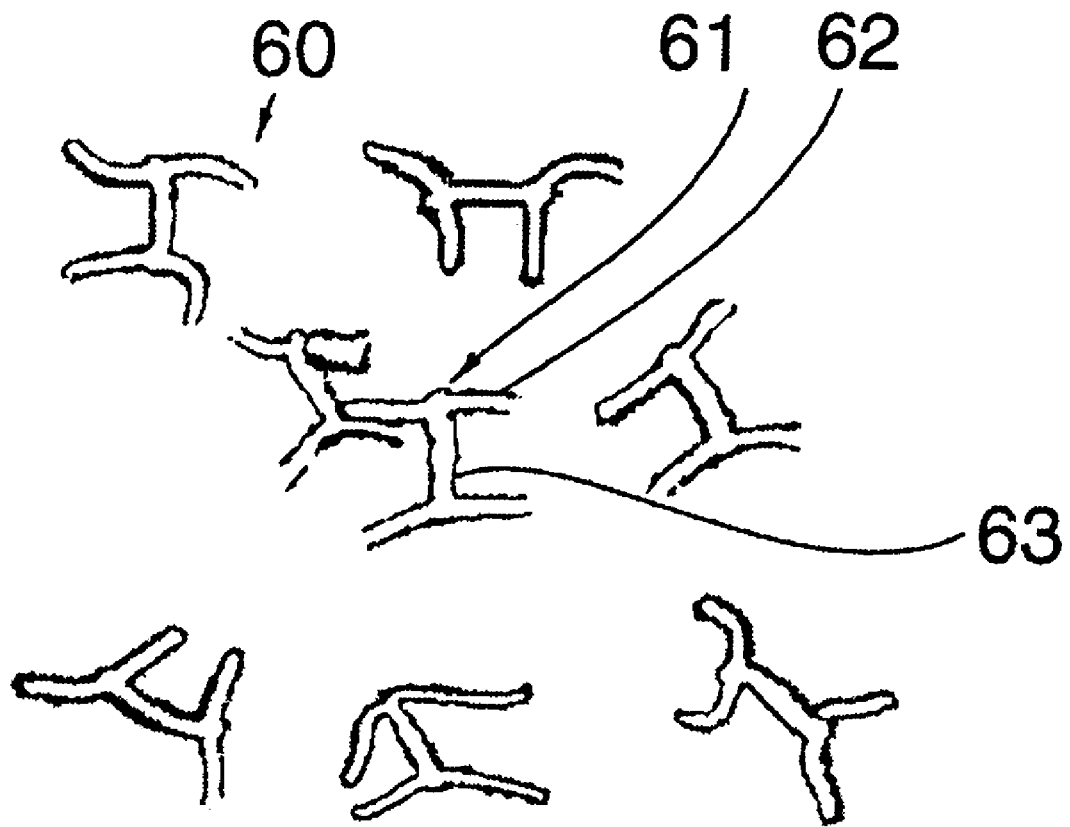


Fig. 6

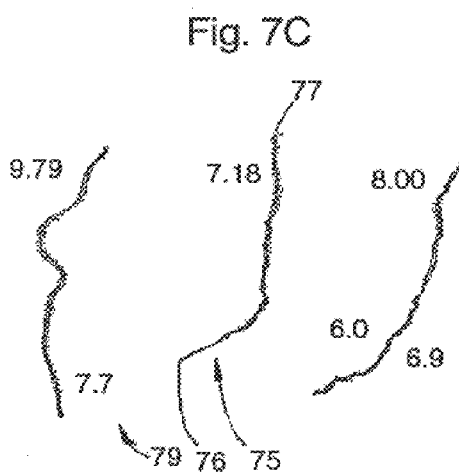
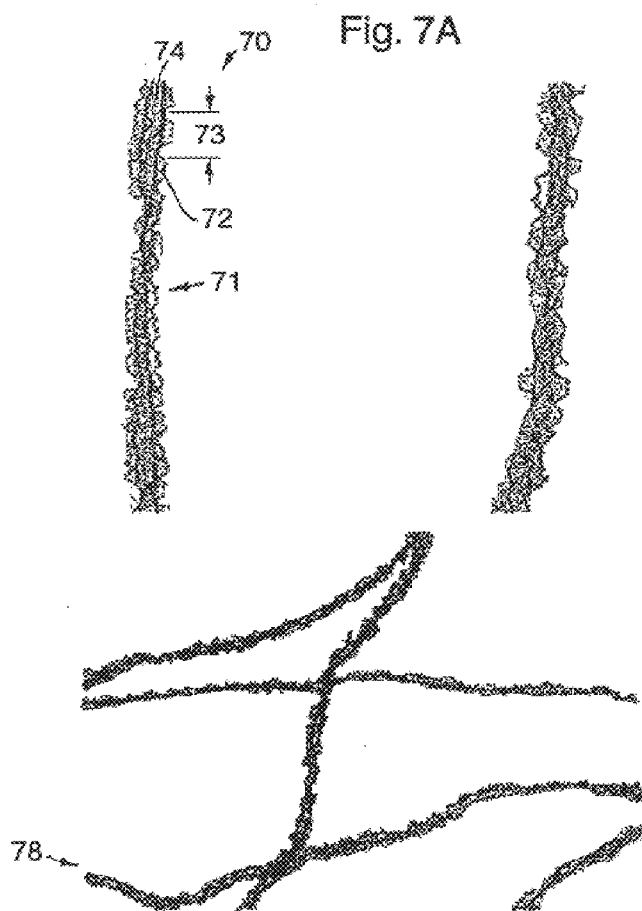


Fig. 7B

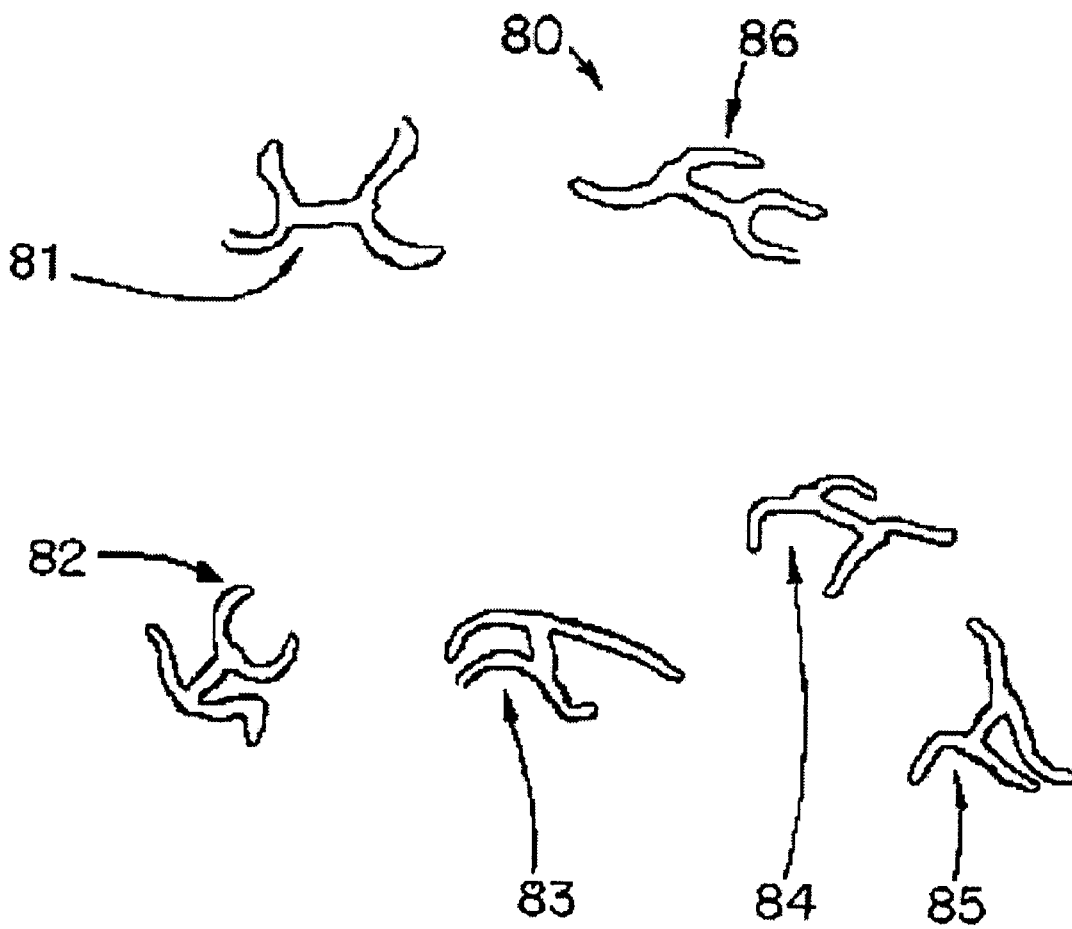
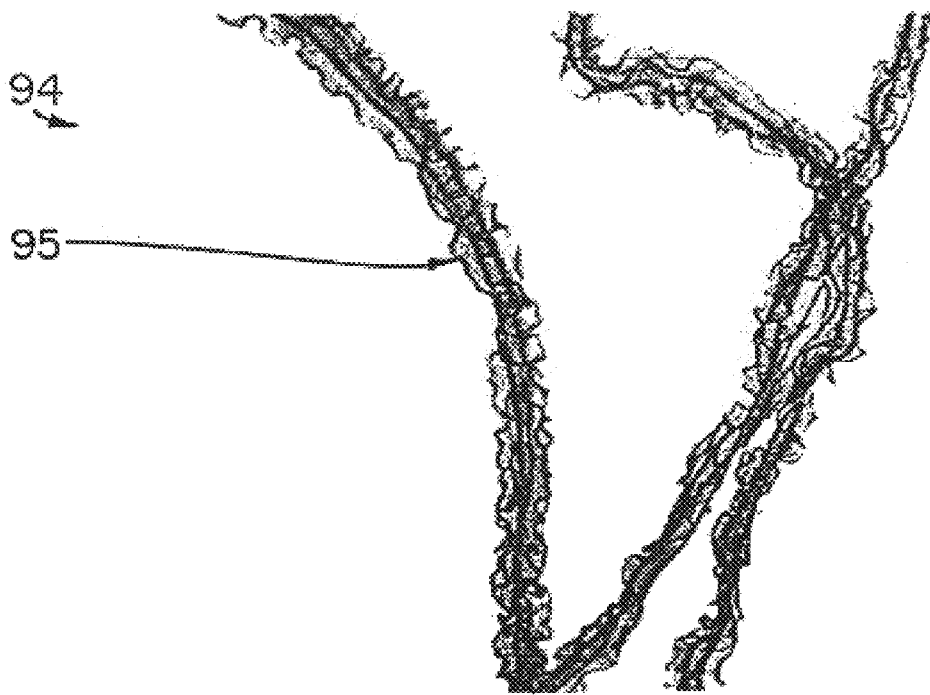
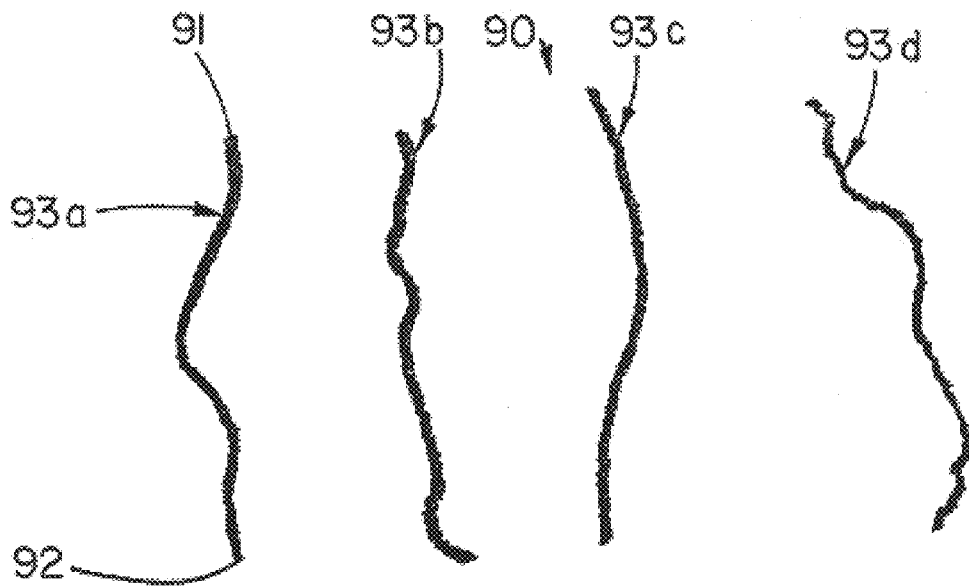


Fig. 8



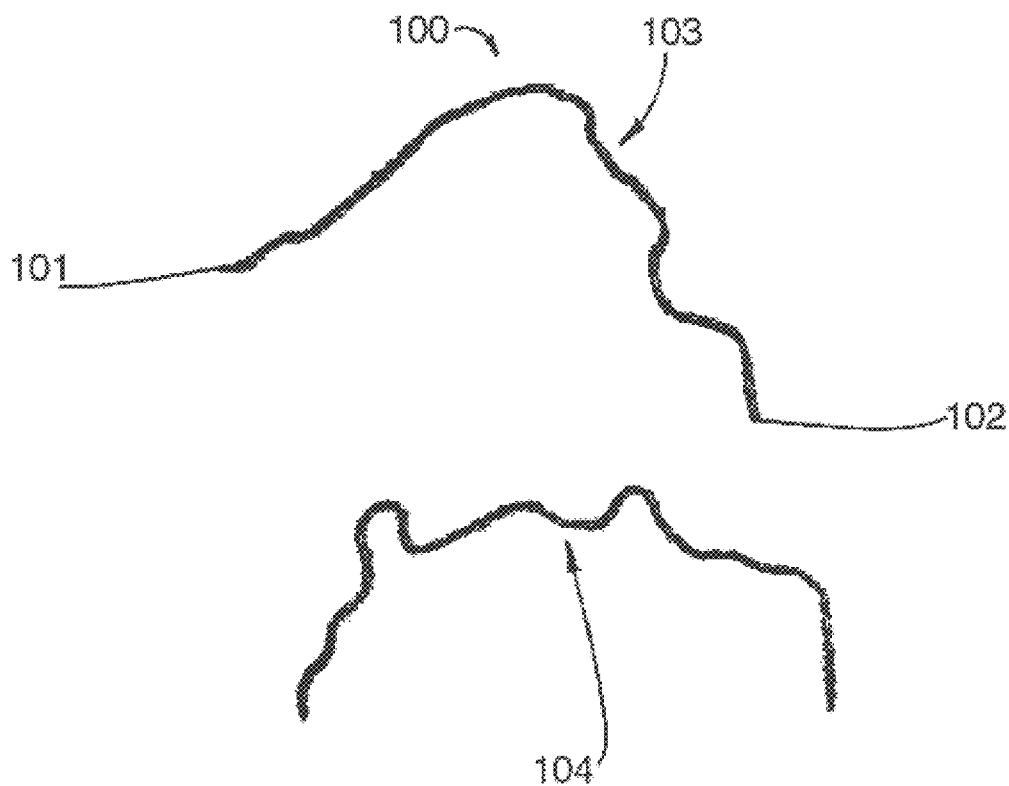


Fig. 10

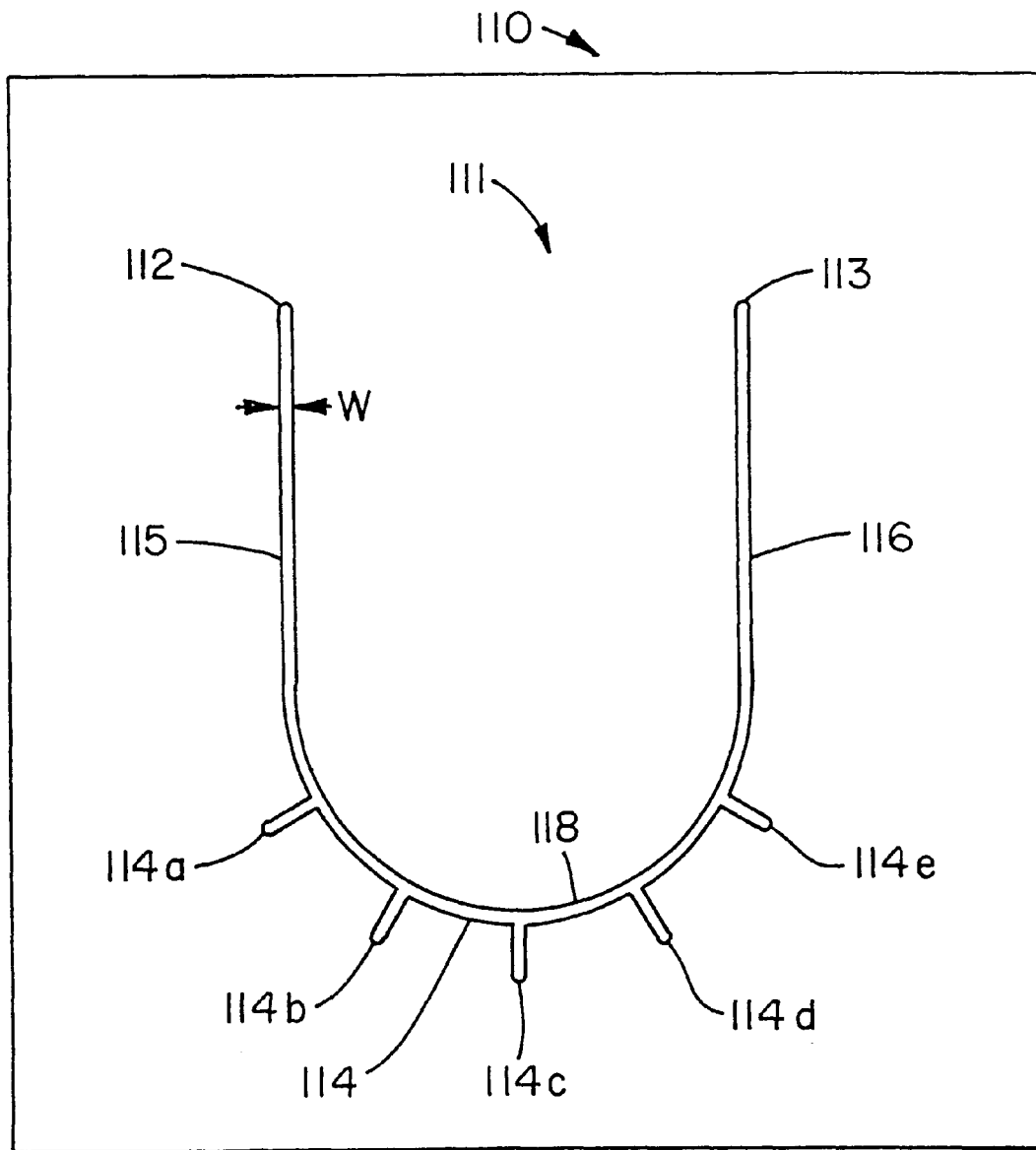


Fig. II

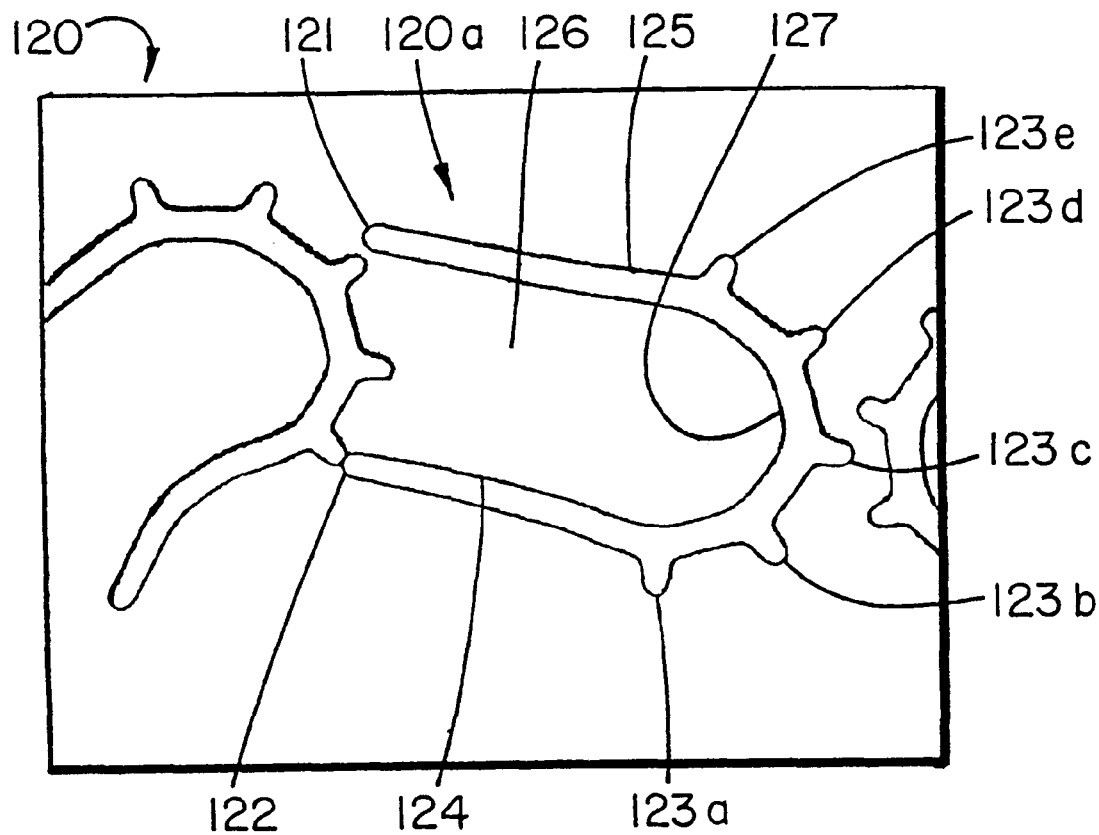


Fig. 12

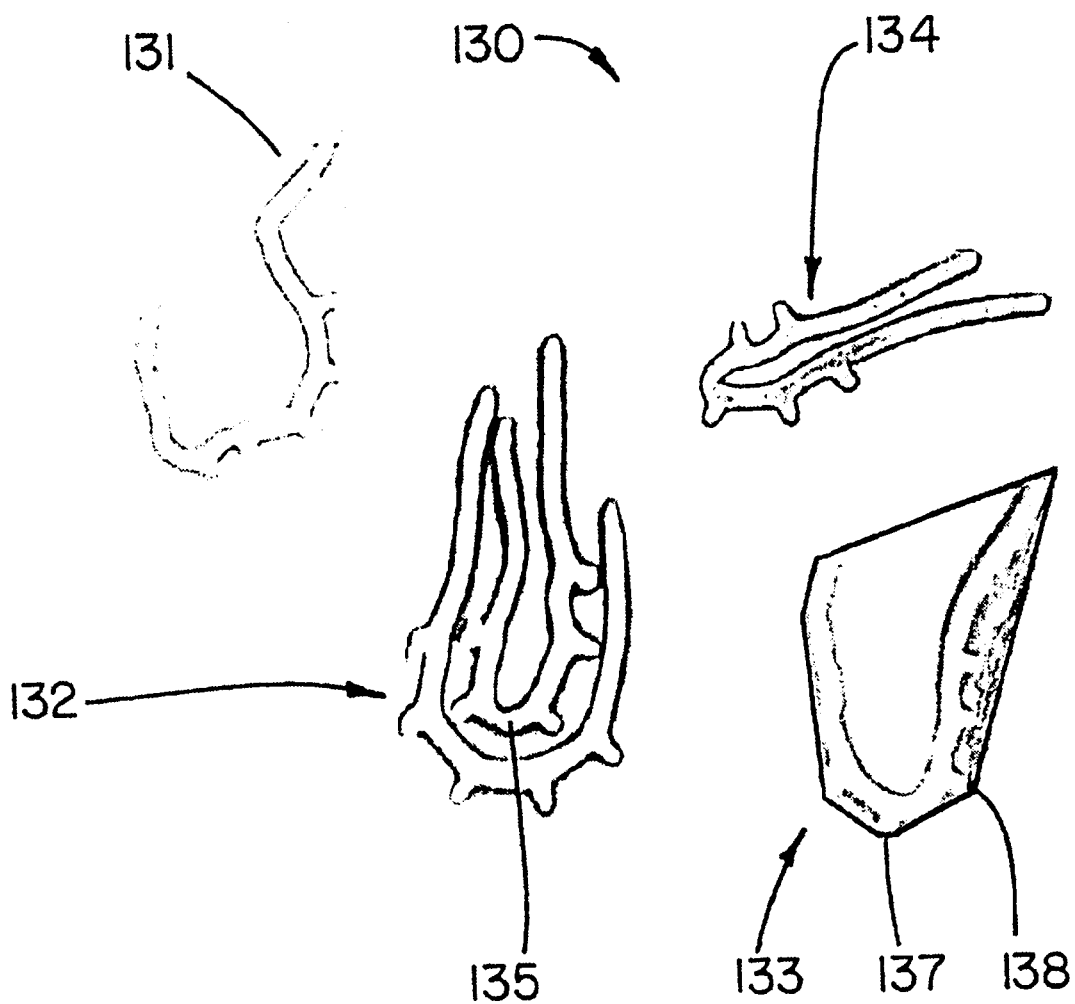


Fig. 13

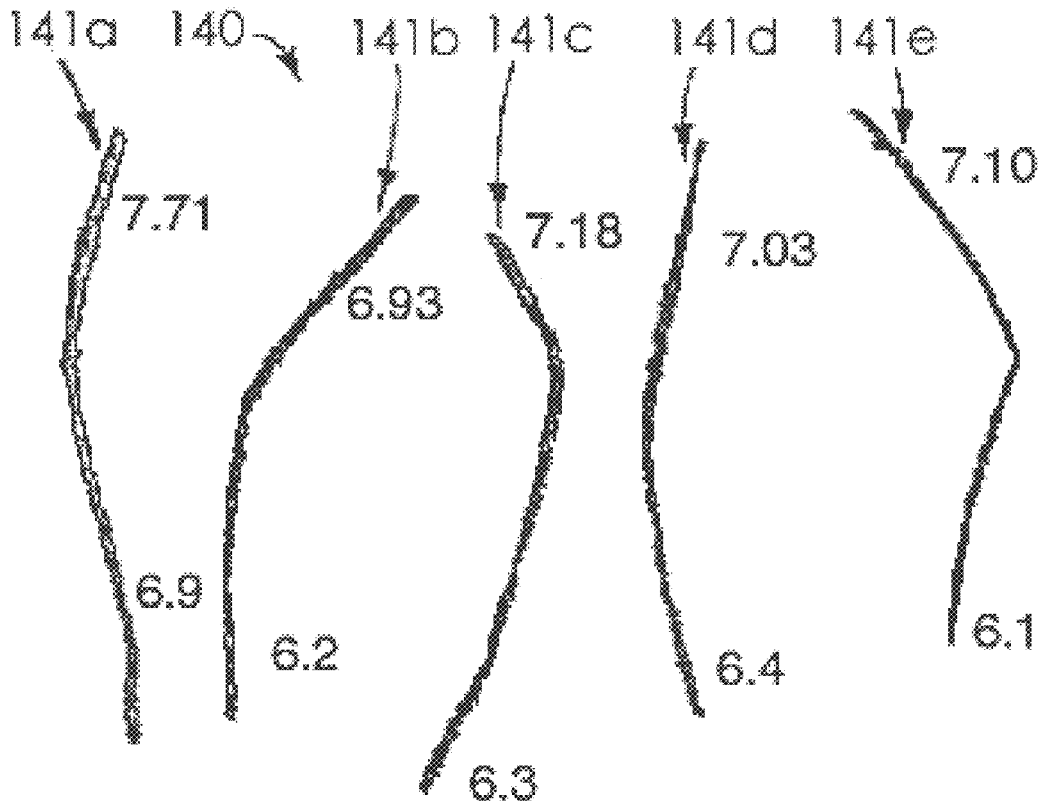


Fig. 14

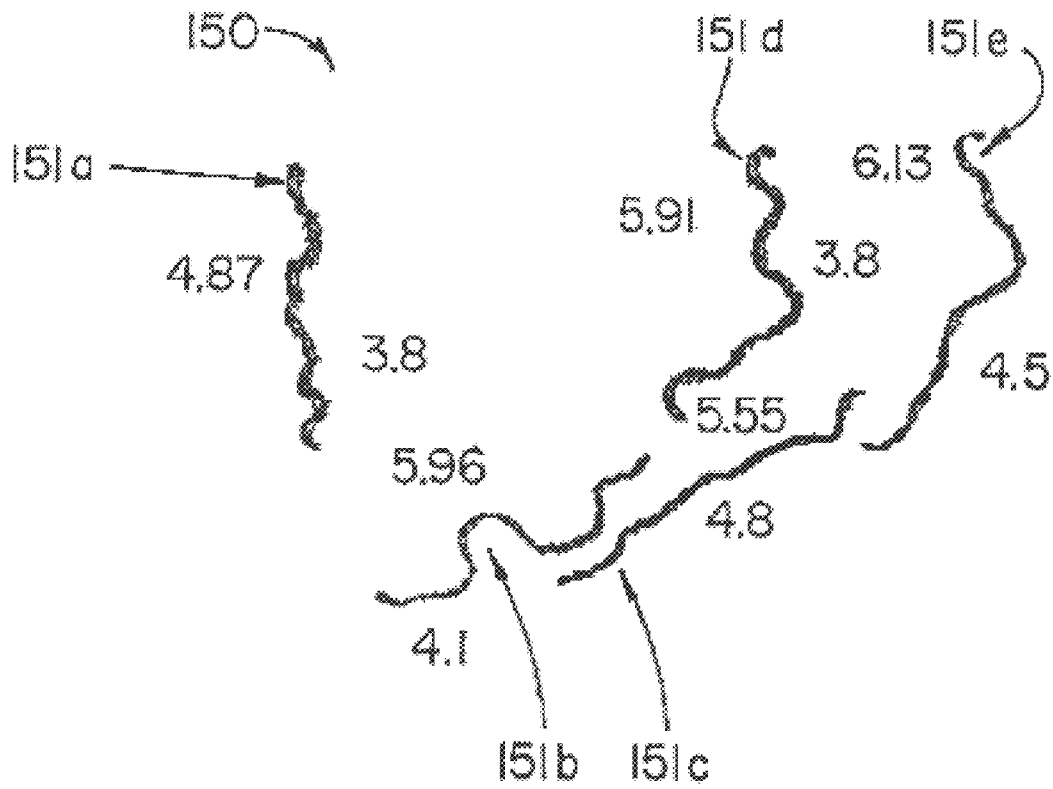


Fig. 15

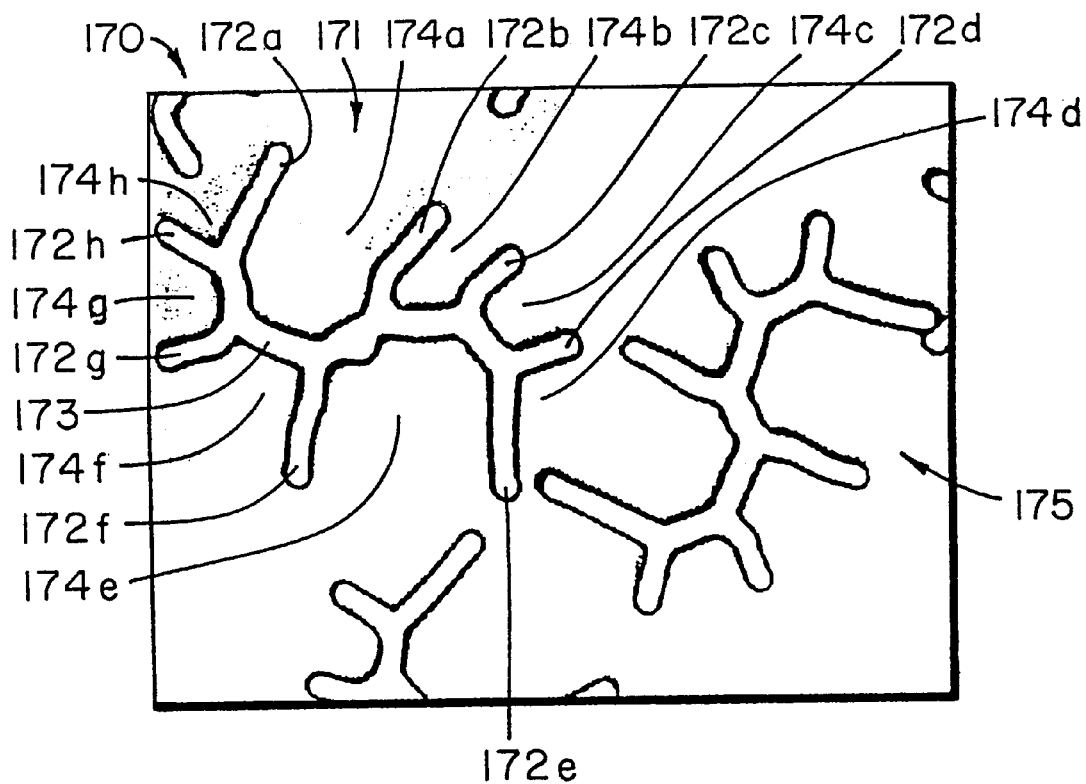


Fig. 17

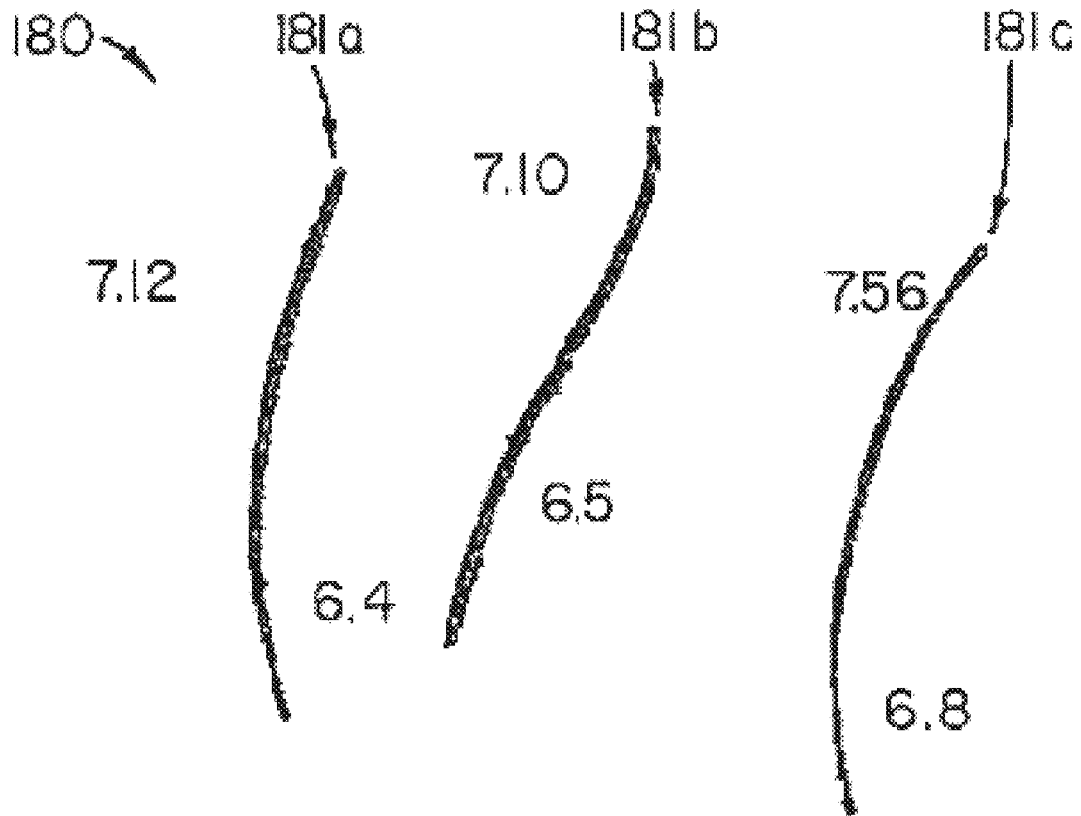


Fig. 18

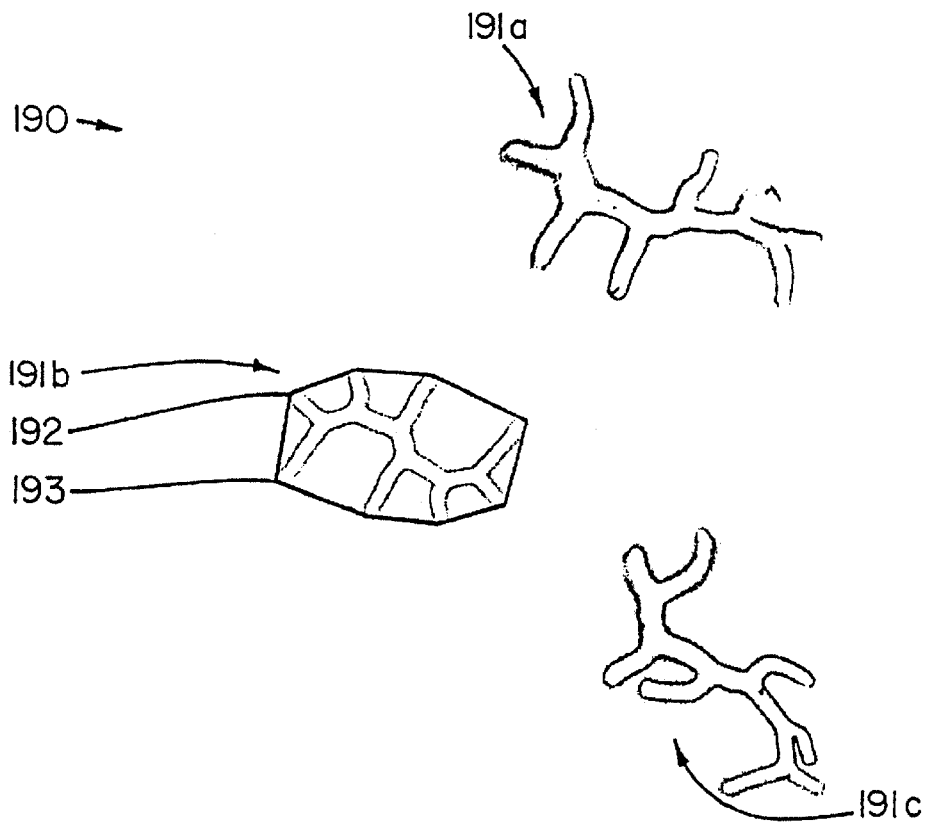


Fig. 19A

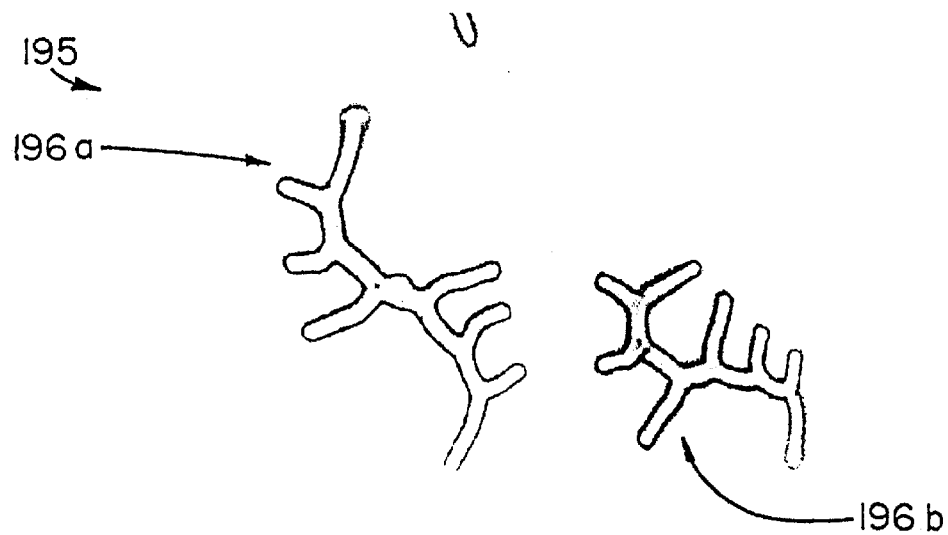


Fig. 19B

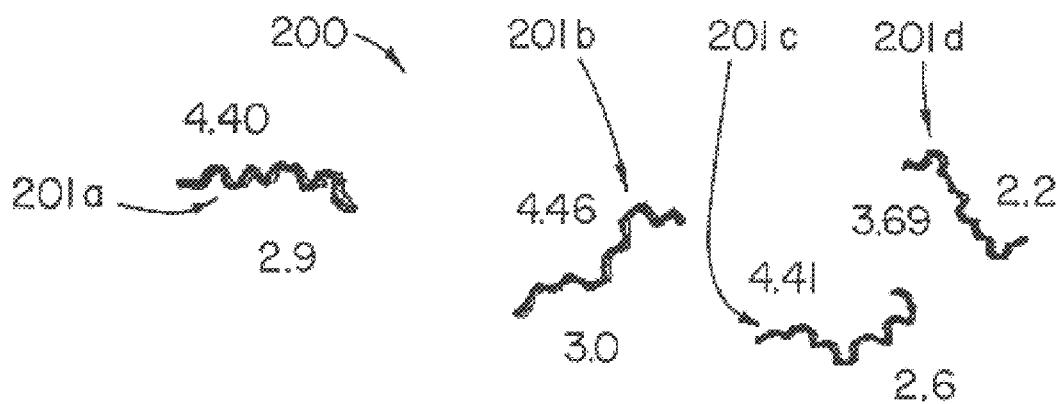


Fig. 20

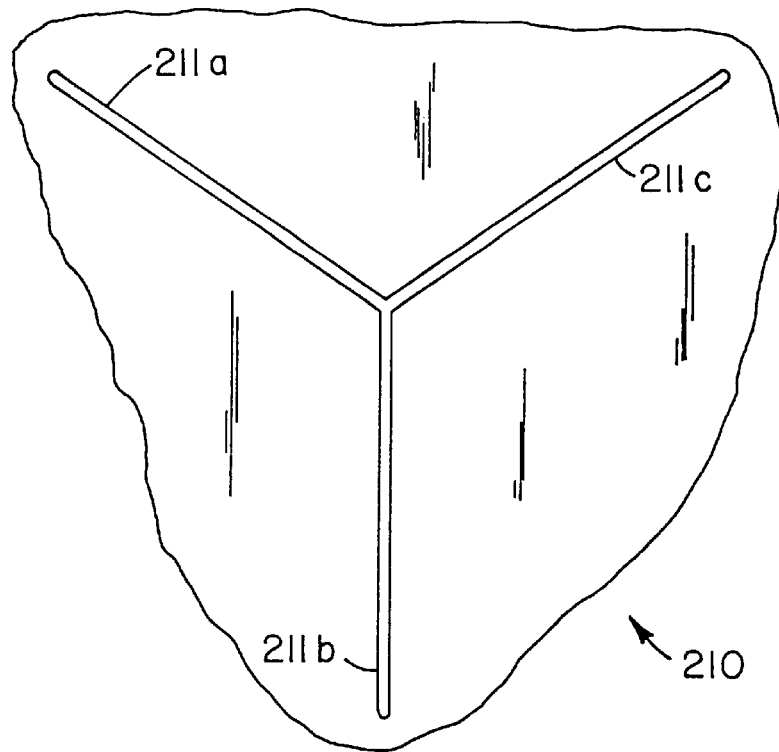


Fig. 21A

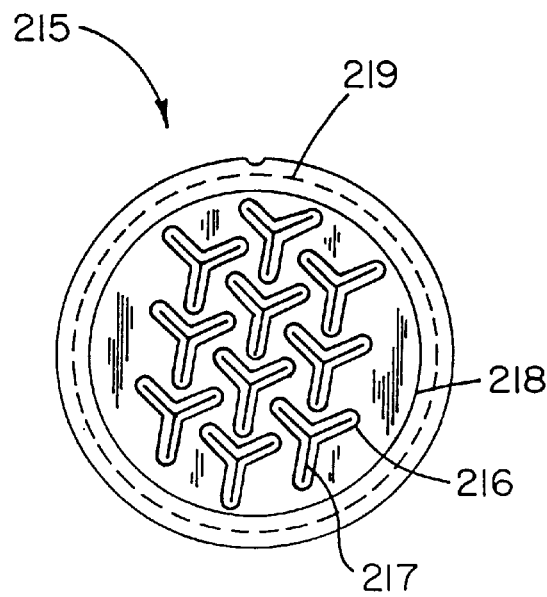


Fig. 21B

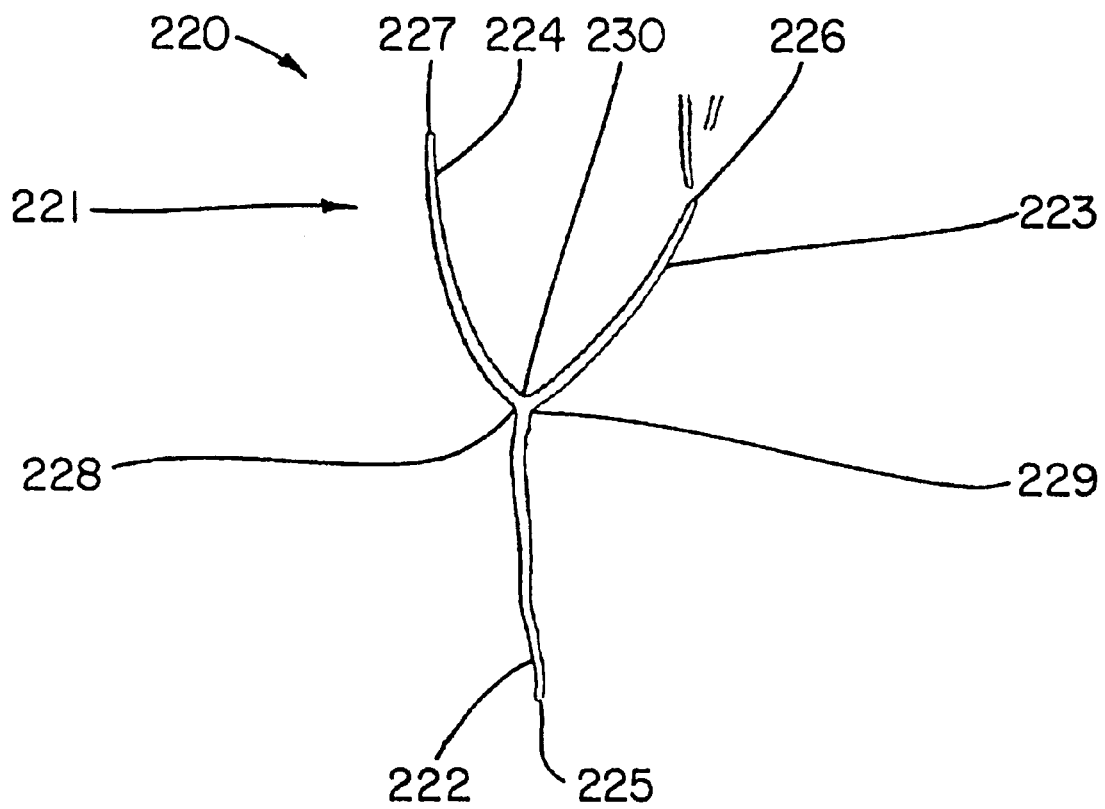


Fig. 22

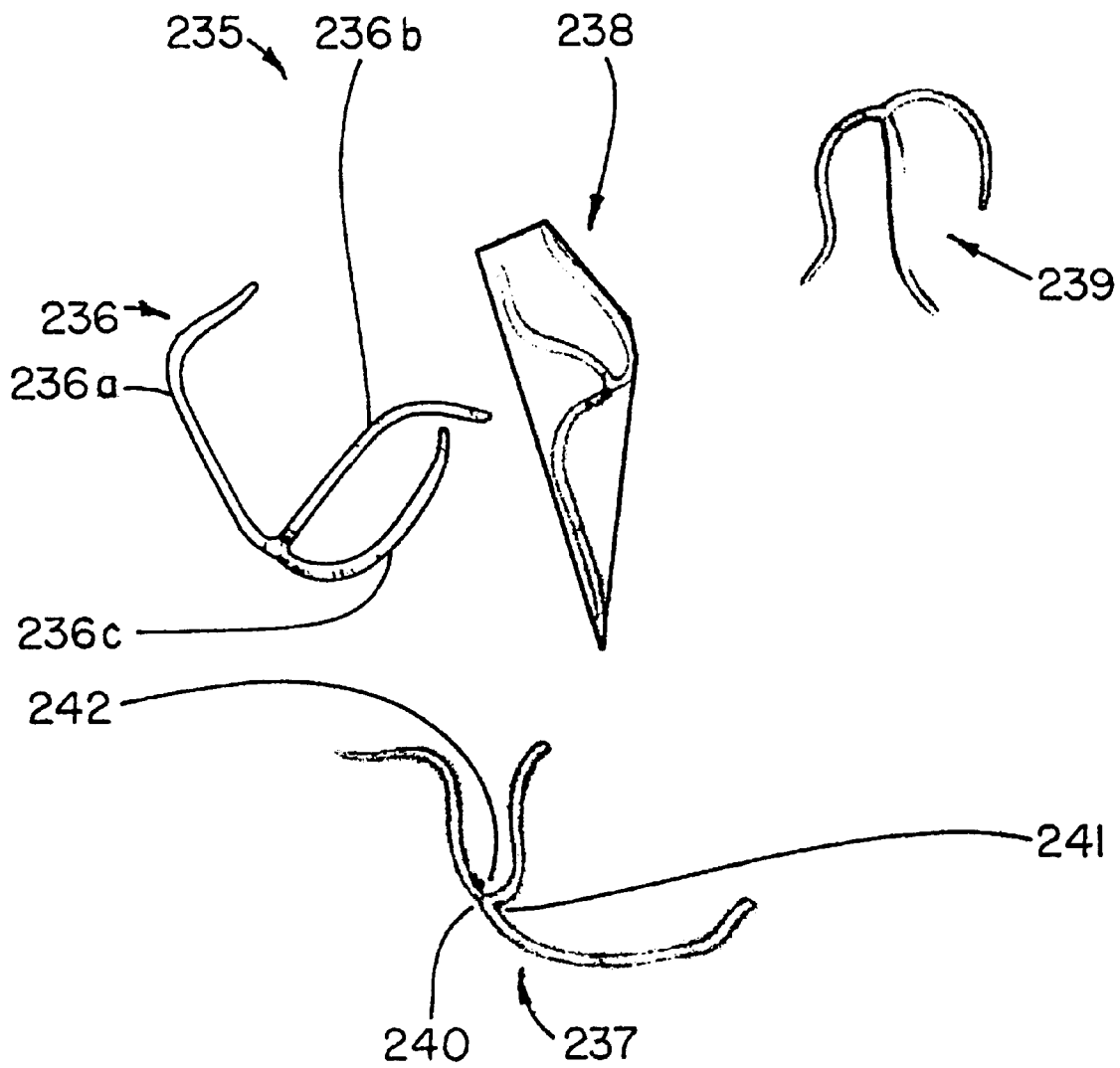


Fig. 23

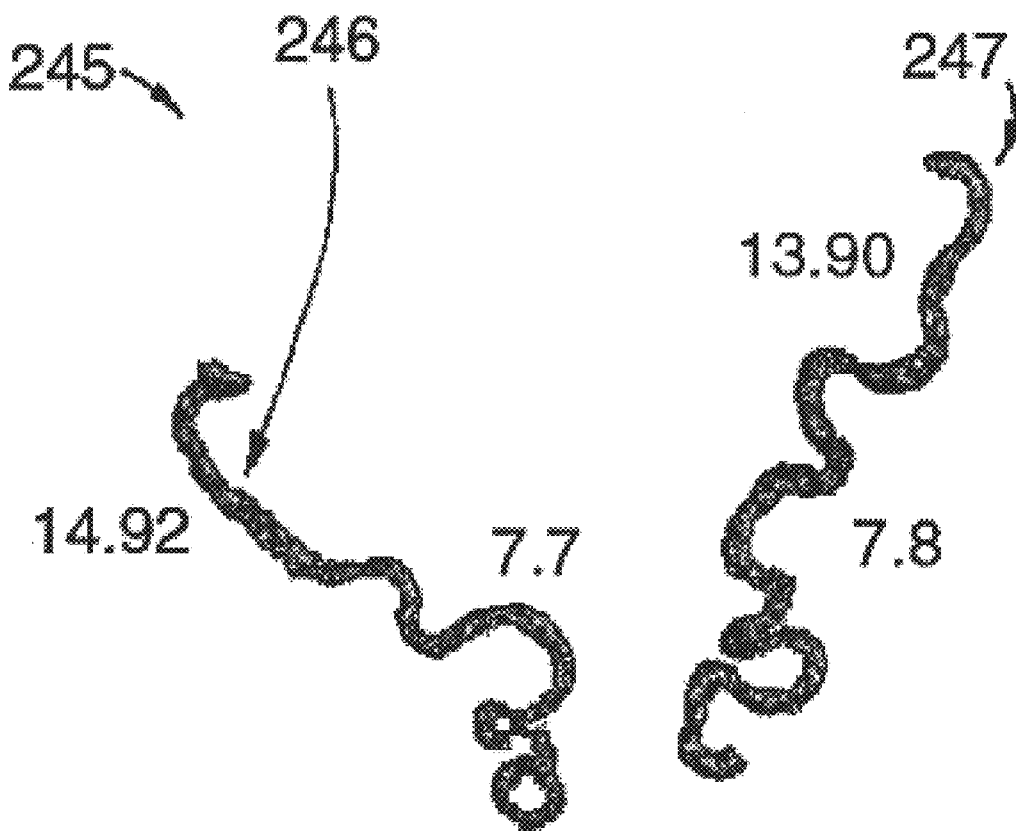


Fig. 24

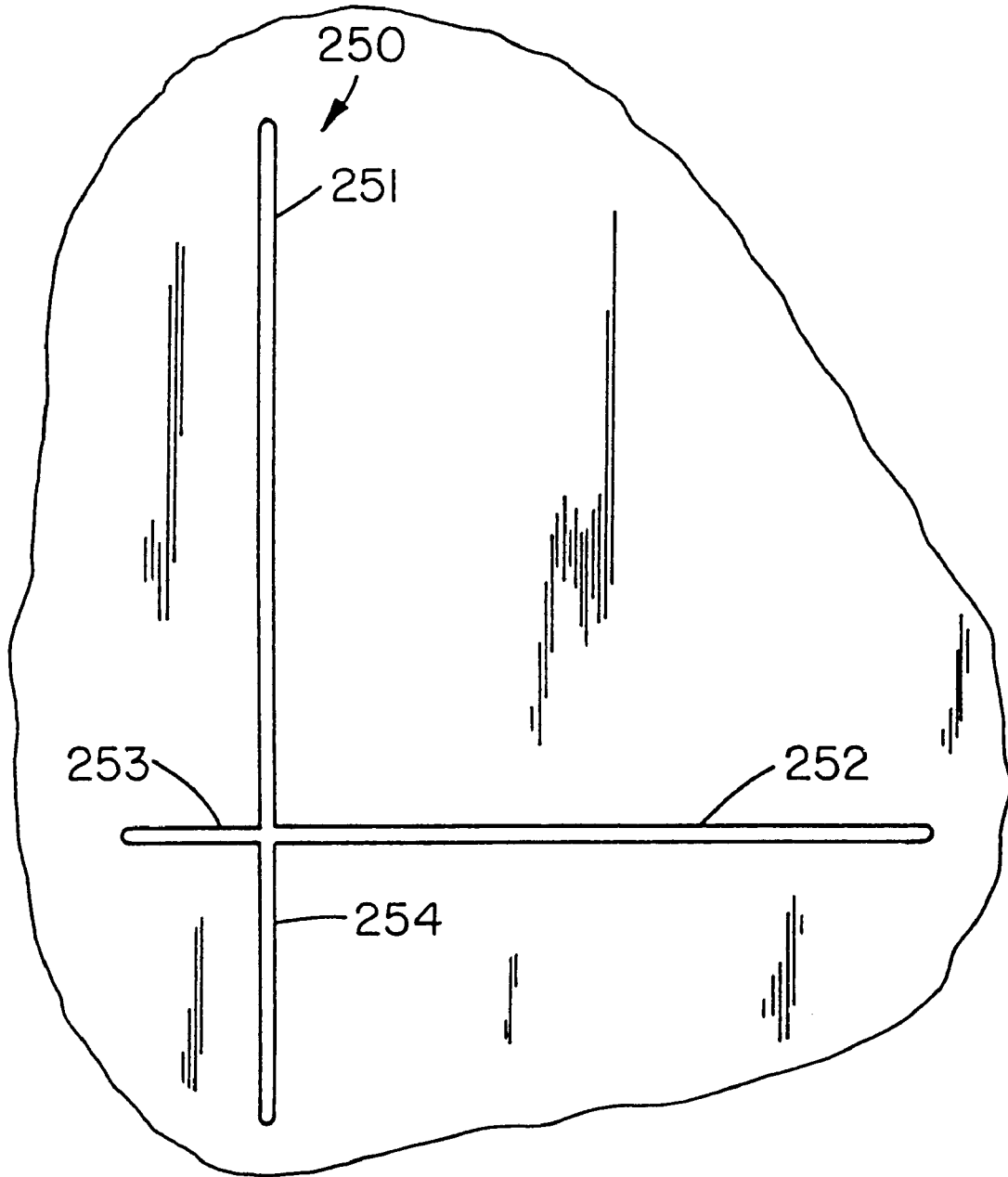


Fig. 25

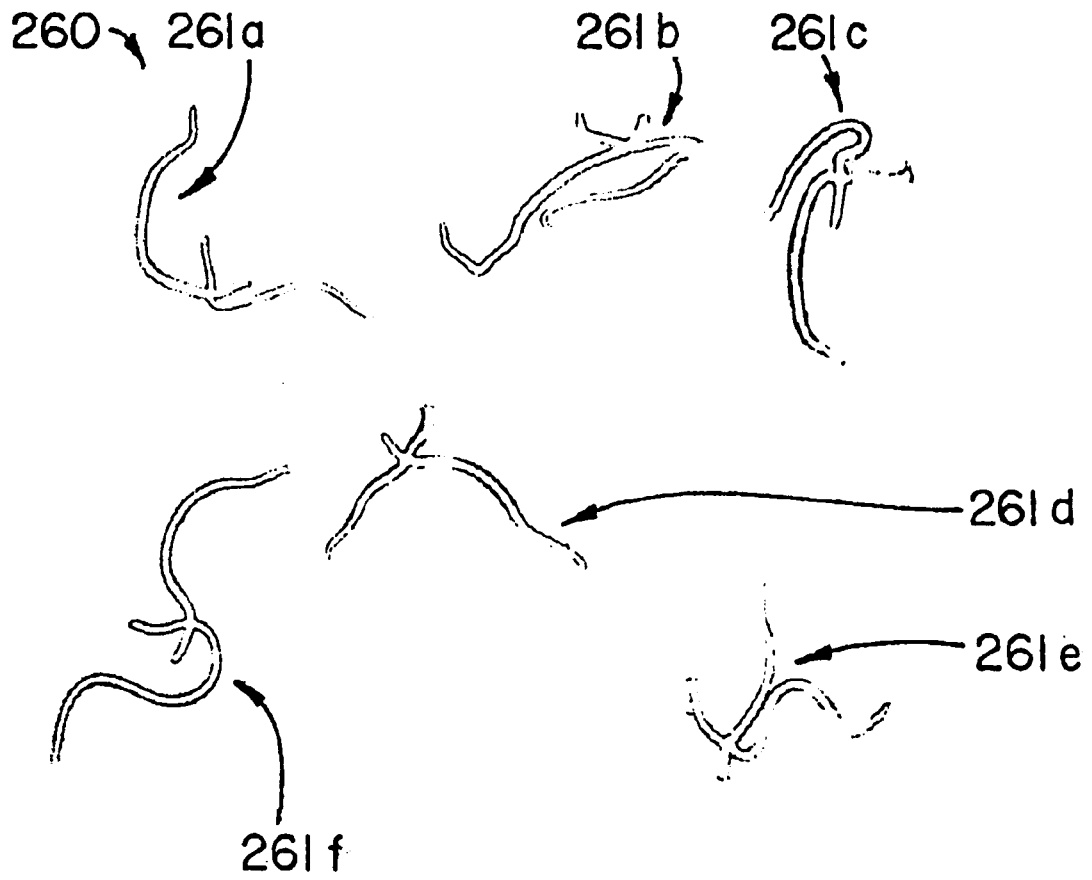
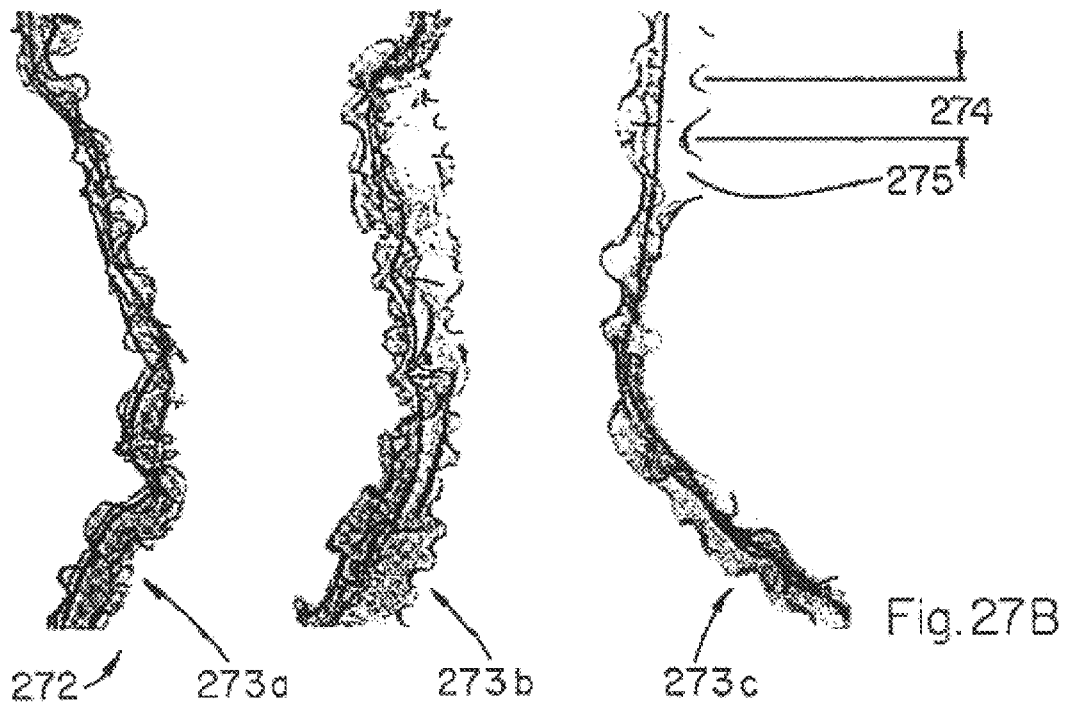
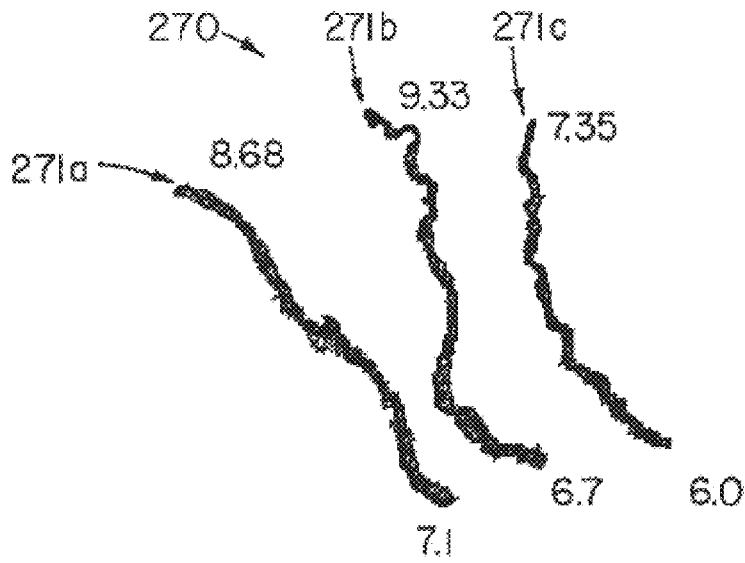


Fig. 26

Fig. 27A



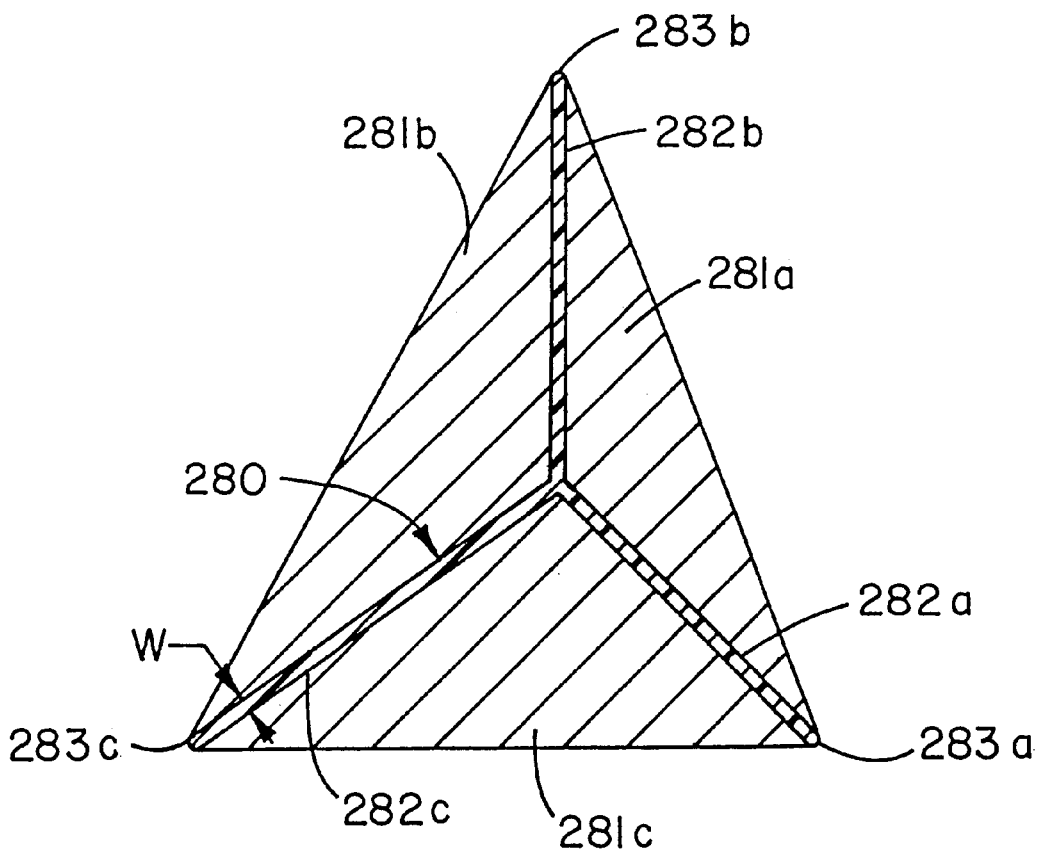


Fig. 28A

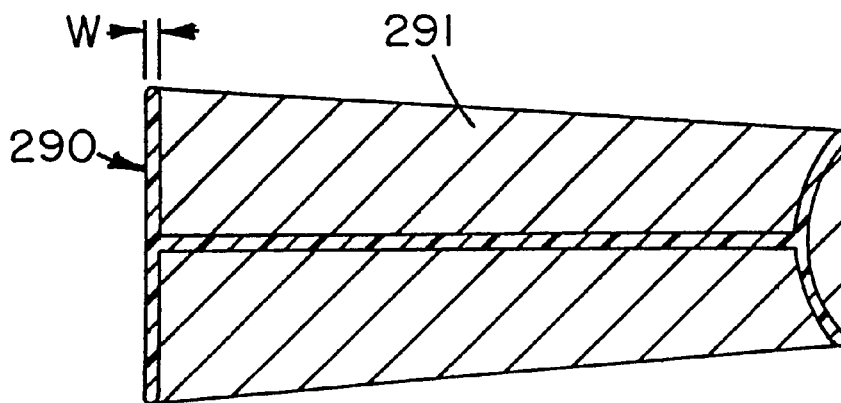


Fig. 28B

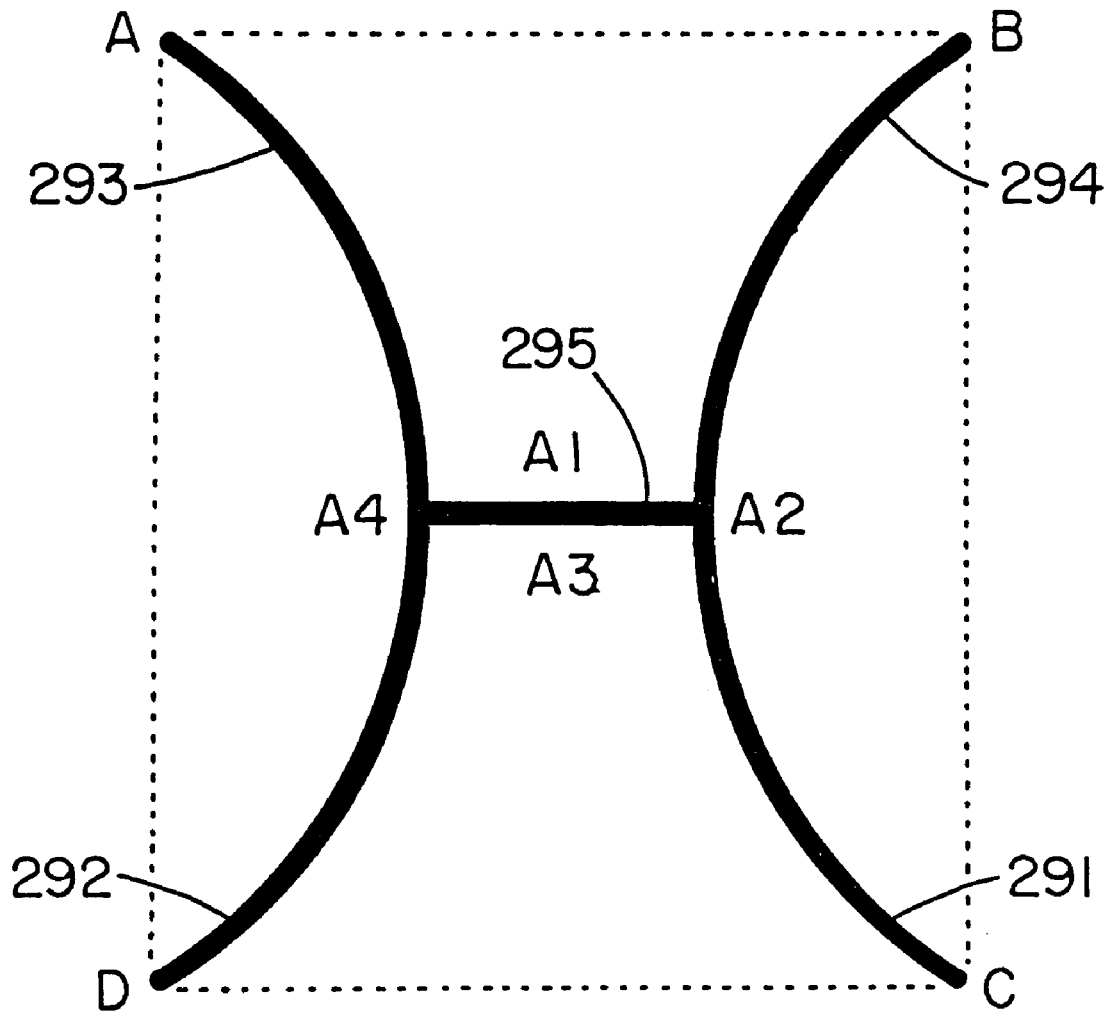
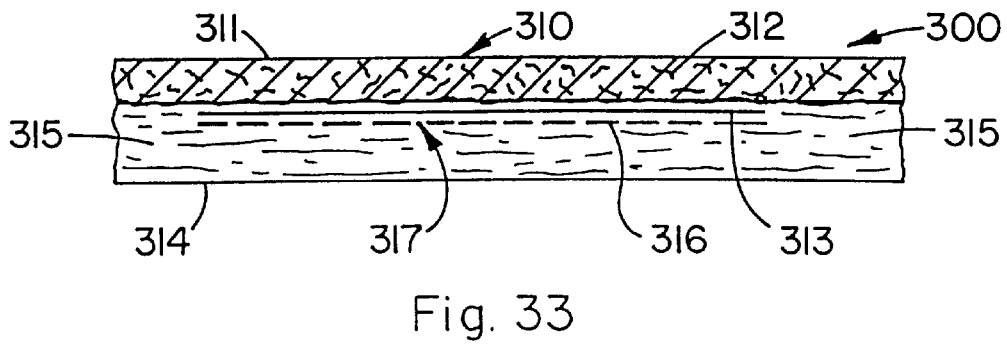
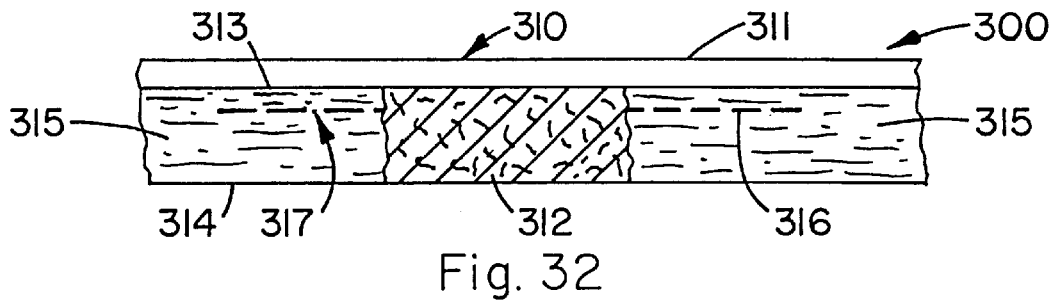
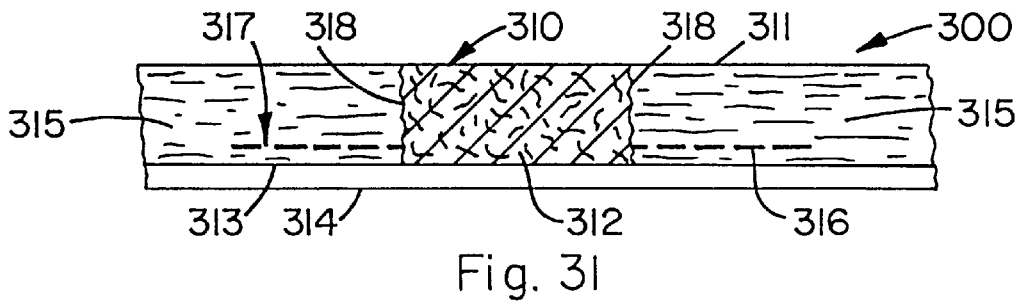
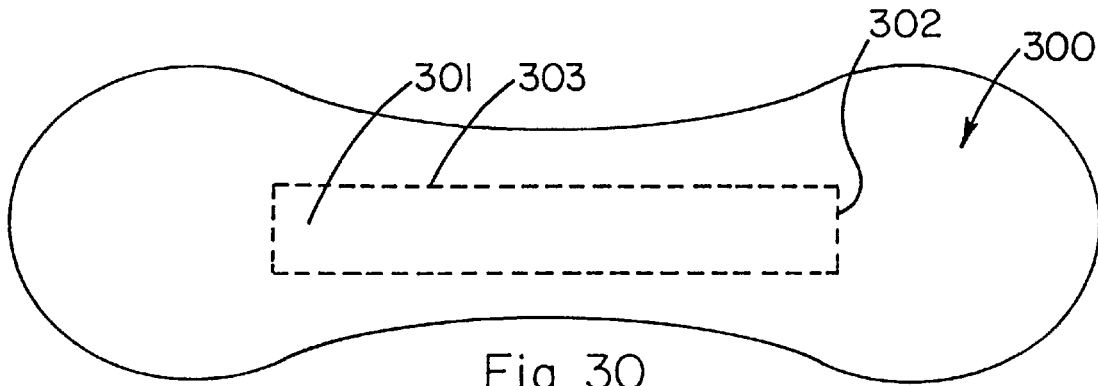


Fig. 29



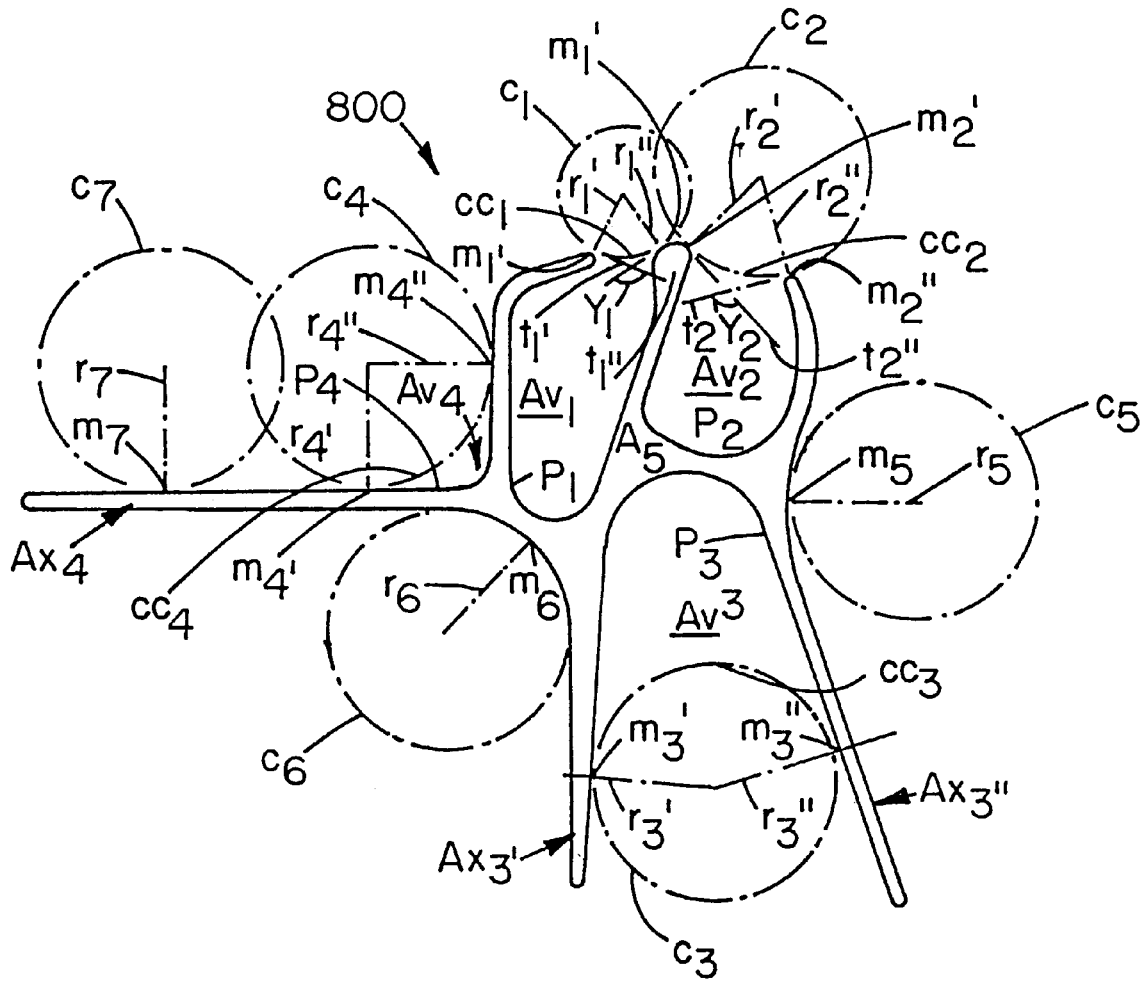


Fig. 34

SYNTHETIC POLYESTER ABSORBENT MATERIALS

This application is a divisional of application Ser. No. 08/916,071, filed Aug. 21, 1997 now U.S. Pat. No. 5,977, 429, which claims the benefit of U.S. Provisional Application Serial No. 60/024,302 filed Aug. 22, 1996.

FIELD OF THE INVENTION

This invention relates to components of absorbent products and absorbent products. More specifically, this invention relates to fibers and structures of the fibers that acquire, distribute and store fluids for use in absorbent products.

BACKGROUND OF THE INVENTION

Cellulose fluff pulp is a common component in the core of disposable absorbent products, such as diapers, catamenials, and incontinent pads. Cellulose fluff pulp is relatively inexpensive. Superabsorbent polymer (SAP) in fiber or powder form is another component that is often found in the core of disposable absorbent products. Core materials like cellulose fluff pulp, chemically modified fluff pulp, or SAP are not easily desorbed because the thermodynamic attraction of aqueous liquids for these materials is extremely high. Hence, liquid in a region containing these materials generally cannot be transported through or away from that region making fluid distribution difficult. Cellulose fluff pulp also collapses when saturated with liquid. This collapse has long been a problem in the absorbent products art limiting their utility.

U.S. Pat. Nos. 4,898,642 to Moore et al.; 4,888,093 to Dean et al.; 4,889,596 to Schoggen et al. and 4,976,819 to Minton describe various chemically modified fluff pulps directed to remedy the deficiencies of untreated fluff pulp.

U.S. Pat. No. 3,219,739 to Breen discloses poly(ethylene terephthalate) (PET) fibers and a process for making those fibers. The fibers disclosed in the '739 patent are characterized by having arms, a relatively high spatial frequency, and relatively short-range sinuous (ruffle) or spiral geometries in the arms. The relatively short range is on the order of ten microns. The fibers disclosed in the '739 patent will not spontaneously transport water. That is, a liquid in contact with the cross-section of a single one of the fibers disclosed in the '739 patent will not continuously spread from the place of contact along the length of the fiber.

U.S. Pat. No. 5,611,981 to Phillips et al. discloses spontaneously wettable fibers having a combination of X values and surface contact angles that satisfy conditions for spontaneous wetting. The X factor is defined therein as $X = P_w / (4r + (\pi - 2)D)$ where P_w is the wetted perimeter of the filament, r is the radius of the circumscribed circle circumscribing the fiber's cross-section, and D is the minor axis dimension across the fiber's cross-section. The teachings of the '981 patent are hereby incorporated herein by reference as if fully set forth herein.

U.S. Pat. No. 5,200,248 to Thompson et al. discloses capillary channel polymeric fibers, which store and transport liquid. The fibers have non-round cross-section shapes which include relatively long thin portions. The cross-section shapes are the same along the length of the fiber. The '248 patent discloses that these capillary channel fibers may be coated with materials that provide an adhesion tension with water of at least 25 dynes/cm. The teachings and especially the definitions in the '248 patent are hereby incorporated by reference as if fully set forth herein.

U.S. Pat. No. 5,268,229 to Phillips et al. discloses fibers having non-round cross-sectional shapes, specifically "U"

and "E" shaped cross-sections with stabilizing legs. These fibers are also spontaneously wettable fibers and have cross-sections that are the same along the length of the fiber.

Co-pending U.S. application titled "Bundles of Fibers Useful for Moving Liquids at High Fluxes and Acquisition/Distribution Structures that Use the Bundles" filed Aug. 15, 1997, discloses bundles of fibers for use as distribution materials. The individual fibers themselves are poor distribution materials having no intra-fiber capillary channels. When combined with each other in bundles, the bundles become excellent distribution materials by utilizing inter-fiber capillary channels. The teachings of and especially the definitions are hereby incorporated herein by reference as if fully set forth herein.

SUMMARY OF THE INVENTION

A highly distorted, bulky synthetic polymeric fiber acquires, distributes and stores fluids when made into an absorbent structure having a large number of the fibers in close proximity to one another. The fibers have a length of between 2 and about 37 millimeters, cross-sections that vary in shape along the length of the fiber, a single fiber bulk factor between 0.5 and 10.0, a short range distortion factor greater than 5, and a long range distortion factor between 0.05 and 0.9. In several preferred embodiments the fiber has at least one cross-section along its length that is characterized as having a distorted "H" shape, a distorted "Y" shape, a distorted "+" shape, a distorted "U" shape, or a distorted shape of a fiber having a cross-section as shown in FIG. 17. The fibers are primarily for use in absorbent products such as diapers, catamenials, and incontinent devices, thus the fibers preferably have an adhesion tension on their surface of greater than 25 dynes/cm with distilled water for adequate movement of aqueous fluids. The fiber surface may be coated with a superabsorbent polymer or a blend of superabsorbent polymer and surfactant.

The absorbent structure comprising the novel fibers of the invention function to manage fluids by temporarily acquiring and distributing fluids. When the novel fibers are coated with a superabsorbent polymer or combined with other materials such as fluff pulp, chemically modified fluff pulp, superabsorbent polymer or combinations thereof, the absorbent structure created functions to permanently store fluids. These absorbent structures have improved water absorbency, decreased wet collapse and reduce water release over many conventional absorbent structures. The absorbent structures in combination with top sheets, distribution layers, shielding layers, storage cores, and back sheets make excellent absorbent products with reduced leakage, improved absorbency and complete utilization of the storage core.

Processes for making the novel fibers of the invention include the step sequences of (1) spinning, optionally drawing, cutting, and shrinking or (2) spinning, optionally drawing, shrinking, and cutting. These processes may be done continuously and at high speeds.

BRIEF DESCRIPTION OF THE DRAWINGS

FIG. 1 is a schematic in plan view of an H-shaped aperture of a spinnerette identified as I-1083 used in Example 1.

FIG. 2 is a photocopy of a photograph at a magnification of 115 (115x) of an as-spun fiber cross-section of Example 1.

FIG. 3 is a photocopy of portions of seven photographs at 111x, each of which shows a cross-section of the novel fibers of the present invention of Example 1.

FIG. 4A is a photocopy of a color photograph at 7× of the novel fibers of Example 1.

FIG. 4B is a photocopy of a color photograph at 40× of the novel fibers of Example 1.

FIG. 5 is schematic in plan view of an H-shaped aperture of a spinnerette identified as I-1042 used in Examples 2 and 19.

FIG. 6 is a photocopy of portions of seven photographs at 285×, each of which shows a cross-section of the novel fibers of the present invention of Example 2.

FIG. 7A is a photocopy of a color photograph at 80× of the novel fibers of Example 2.

FIG. 7B is a photocopy of a color photograph at 36× of the novel fibers of Example 2.

FIG. 7C is a photocopy of a color photograph at 7× of the novel fibers of Example 2.

FIG. 8 is a photocopy of portions of six photographs at 285×, each of which shows a cross-section of the novel fibers of the present invention of Example 3.

FIG. 9A is a photocopy of a color photograph at 7× of the novel fibers of Example 3.

FIG. 9B is a photocopy of a color photograph at 40× of the novel fibers of Example 3.

FIG. 10 is a photocopy of a color photograph at 7× of novel fibers of the present invention of Example 4.

FIG. 11 is a schematic in plan view of a U-shaped aperture of a spinnerette identified as I-1127 used in Examples 12 and 13.

FIG. 12 is a photocopy of a photograph at 464× of an as spun fiber cross-section of Example 12.

FIG. 13 is a photocopy of portions of four photographs at 285×, each of which shows a cross-section of the novel fibers of the present invention of Example 12.

FIG. 14 is a photocopy of a color photograph at 7× of the novel fibers of Example 12.

FIG. 15 is a photograph at 7× of the novel fibers of the present invention of Example 13.

FIG. 16 is a schematic in plan view of an aperture of a spinnerette identified as I-1004 used in Example 14, the shape of the aperture hereinafter called "4DG".

FIG. 17 is a photocopy of a photograph at 464× of an as-spun fiber cross-section of Example 14.

FIG. 18 is a photocopy of a color photograph at 7× of the novel fibers of the present invention of Example 14.

FIG. 19A is a photocopy of portions of three photographs at 285×, each of which shows a cross-section of the novel fibers of the present invention of Example 15.

FIG. 19B is a photocopy of portions of two photographs at 285×, each of which shows a cross-section of the novel fibers of Example 15.

FIG. 20 is a photocopy of a color photograph at 7× of the novel fibers of Example 15.

FIG. 21A is a schematic in plan view a Y-shaped aperture of a spinnerette identified as I-1195 used in Example 20.

FIG. 21B is a schematic plan view of a face of the spinnerette I-1195 showing a plurality of the Y-shaped apertures.

FIG. 22 is a photocopy of a photograph at 115× of an as-spun fiber cross-section of Example 20.

FIG. 23 is a photocopy of portions of four photographs at 115×, each of which shows a cross-section of the novel fibers of the present invention of Example 20.

FIG. 24 is a photocopy of a color photograph at 7× of novel fibers of Example 20.

FIG. 25 is a schematic in plan view of an aperture of a spinnerette identified as I-1198 used in Example 21.

FIG. 26 is a photocopy of portions of six photographs at 115×, each of which shows a cross-section of the novel fibers of the present invention of Example 21.

FIG. 27A is a photocopy of a color photograph at 7× of the novel fibers of Example 21.

FIG. 27B is a photocopy of a color photograph at 40× of the novel fibers of Example 21.

FIG. 28A is a schematic of a cross-section of a fiber for use in illustrating the definition of the single fiber bulk factor.

FIG. 28B is a schematic of a cross-section of a fiber for use in illustrating the definition of the single fiber bulk factor.

FIG. 29 is a schematic cross-section of a fiber useful in defining the short-range distortion factor (SRDF).

FIG. 30 is a schematic top plan view of an absorbent article.

FIG. 31 is a partial side sectional view of a preferred embodiment of an absorbent article utilizing the absorbent structures of the present invention.

FIG. 32 is a partial side sectional view of another preferred embodiment of an absorbent article utilizing the absorbent structures of the present invention.

FIG. 33 is a partial side sectional view of still another preferred embodiment of an absorbent article utilizing the absorbent structures of the present invention.

FIG. 34 is a schematic cross-section of a fiber used in defining SCV and SCSA.

FIG. 35 is a schematic cross-section of a fiber used in defining S and CCW.

DETAILED DESCRIPTION OF THE INVENTION

Novel absorbent structures are made of a plurality of novel fibers in proximity to each other. The novel fibers are short, highly distorted having varying cross-section shapes along their lengths, and bulky. The absorbent structures provide fluid management properties functioning to either temporarily acquire and distribute fluids or permanently store fluids. The fluid management properties depend on the type of novel fibers utilized in the absorbent structures. The absorbent structures are used in absorbent products, such as diapers, catamenials, or incontinent devices.

The novel fibers are short meaning that each fiber has a length along its axis of between about 2 and about 37 millimeters, preferably between about 2 and 19 millimeters.

The novel fibers are bulky meaning that each fiber has a single fiber bulk factor (SFBF) of between 0.5 and 10.0, preferably between 1.5 and 7.5. The examples represent SFBF of between 0.5 and 4.0. SFBF is a measure of the ratio of void areas formed by the cross-section of the fiber to the polymer area of the cross-section of the fiber. The void areas are illustrated in the fiber cross-sections of FIGS. 28A–B along with exemplary calculations as discussed below. Since the novel fibers have varying cross-sections along their length, the SFBF is an average of 50 cross-section measurements.

Bulkiness may also be expressed as a function of the as spun fiber. "As spun" means the state of the novel fibers prior to the step of shrinking or drawing. The as spun fibers

have non-round cross-section shapes and include those fibers disclosed in U.S. Pat. Nos. 5,200,248; 5,268,229 and 5,611,981 and in co-pending U.S. application titled "Bundles of Fibers Useful for Moving Liquids at High Fluxes and Acquisition/Distribution Structures that Use the Bundles" filed Aug. 15, 1997. In combining the teachings of the above references, the as spun fibers may be characterized by the following two classifications:

1. The fibers are those classified as having "good" capillary channels on their surface such that the fibers have (a) a Specific Capillary Volume of at least 2.0 cc/g and a Specific Capillary Surface Area of at least 2000 cm²/g, or (b) a Slenderness Ratio of at least 9 and at least 30 percent of intra-fiber channels with a capillary channel width of less than 300 microns.

2. The fibers are those classified as having "poor" or no capillary channels on their surface such that the fibers have (a) a Specific Capillary Volume of less than 2.0 cc/g or a Specific Capillary Surface Area of less than 2000 cm²/g, and (b) a Slenderness Ratio of less than 9 or more than 70% of intra-fiber channels with a capillary channel width of greater than 300 microns. Preferably, these as spun fibers have a SFBF of greater than 4.0.

Details of measuring the parameters set forth above for the as spun fibers are discussed below.

The novel fibers are highly distorted having a highly variable cross-section shapes caused by a sinuous or ruffled character of arms of the fiber or walls of channels of the fiber relative to the backbone or spine of the fiber from which the arms or the walls project. That is, the arms or walls of the cross-section of the fibers are highly distorted. The distorted shape in this context is created from the shape of an as spun fiber that has undergone the step of shrinking. During shrinking, the cross-section shape of the as spun fiber distorts. Channels refers to the ruffled walls coupled with a base defining one or more channels.

Distortions of the novel fiber of the present invention are characterized by a short range distortion factor (SRDF) for the arms of the fiber or the walls of the channels and a long-range distortion factor (LRDF) for the length, i.e. backbone, of the fiber. The SRDF is greater than 5.0, preferably between 5 and 70, and more preferably between 18 and 36. The LRDF is between 0.05 and 0.9, preferably between 0.1 and 0.6. Examples herein represent SRDF of between 11 and 66 and LRDF of between 0.10 and 0.49.

The SRDF is defined as the percent of the coefficient variation of the ratio of the area of channels C_{area} to the area of the cross-section of the fiber material M_{area} for fifty measurements on randomly selected cross-sections of the fibers. Thus,

$$SRDF=100 \times (\sigma/X)$$

wherein X equals the average (C_{area}/M_{area}) for measurements on fifty cross-sections and σ equals the standard deviation of the 50 values for (C_{area}/M_{area}).

FIG. 29 illustrates a fiber cross-section and is useful in explaining how the channel area of a fiber is calculated. For any cross-section, the channel area C_{area} is determined by first enclosing the cross-section in a polygon whose segments are tangent to two points on the cross-section and intersect at angles interior to the polygon of less than 180 degrees. The polygon is demonstrated in FIG. 29 as the dotted line segments. Each channel area is defined by the surfaces of the cross-section of the fiber and the line segments tangent to the two points on the cross-section. In FIG. 29 the line segment AB and surfaces of the two arms 293, 294, and the base 295 of the fiber delimit the channel area

A1. Similarly, the line segment BC and surfaces of the two arms 291, 294 delimit the channel area A2. All channel areas are included in the value for C_{area} for cross-section of a fiber. Thus, the value of C_{area} is equal to the sum of the area of channels A1+A2+A3+A4. The fiber material area M_{area} is the area of the cross-section of the fiber, which includes the area of the arms 291-294 and the base 295. For each cross section, the ratio of C_{area} to M_{area} is determined. The average and the standard deviation of the ratio of the C_{area} to M_{area} is determined for fifty cross sections. Once the average and the standard deviation have been measured, the SRDF is calculated.

LRDF is a function of L_1 and L_0 . L_0 is the average length along the backbone or spine of the novel fiber. L_1 is the diameter of the circle circumscribing the novel fiber. L_0 and L_1 are measured using photomicrographs. The fibers are placed on a microscope slide and a photomicrograph at a known magnification, such as a magnification of about 7, is taken. The lengths L_1 and L_0 , while measured from the photomicrograph, are the actual lengths of the backbone and diameter, respectively. These lengths may be approximated using a ruler. Alternatively, a computer imaging and measurement system may be used to determine L_0 , L_1 , and LRDF.

In one embodiment as utilized by the examples below, the computer based imaging and measurement system to determine LRDF includes an optical system for obtaining images of the fiber, which is programmed with algorithms for measuring lengths of the fiber, and a printer for making copies of the fiber images. The optical system includes an illuminated base, a video camera equipped with a macro lens, and a conventional personal computer that includes an image grabber board. The width of the field of view for each image is preferably at least 15 millimeters at the desired magnification allowing for the entire length of the novel fibers to be in the field of view. Verification of the magnification in the image is done using a ruler in the field of view and an algorithm that sets the scale in the image field based upon the distance between points identified in the field of view.

Various algorithms can be used in the measuring system to determine L_0 and L_1 . The determination of L_0 may be accomplished by tracing the insertion point along the length of the image of the fiber using an input/output mouse type of device. Alternatively, the ends of the image of the fiber can be identified using a mouse type device and the computer can be instructed to run an algorithm to determine the length of the fiber based upon the identification of the two end points and fiber image in the image field. L_1 can also be determined with the aid of the measuring system. The distal points of the fiber can be identified and the length between those points equated with the diameter of the circumscribing circle. Alternatively, the points in the image field corresponding to the fiber can be identified by the computer, and the computer can run an algorithm to fit a circle around the fiber that circumscribes the fiber.

To provide bulkiness and distortion, the shape of the cross-section of the novel fibers may be distorted "H", "Y", "+", or "U" shapes as shown in the Examples. The novel fiber cross-section shape may also be a distorted shape of the as spun fiber shown in FIG. 17. The shape of the as spun fiber in FIG. 17 has been commercially referred to as "4DG", available from Eastman Chemical Company of Kingsport, TN. Of course, the as spun fiber cross-section shapes are the non-distorted "H", "Y", "+", "U" or "4DG" shapes.

The fibers have a denier of between 3 and 100 dpf and more preferably between 3 and 30 dpf. Denier (dpf) is the

average denier of the individual fiber measured in grams of fiber per 9000 meters of the individual fiber.

Preferably, the novel fibers of the invention are made from a polyester, such as poly(ethylene terephthalate). However, the novel fibers may also be formed from other polymers that shrink significantly when heated such as polystyrene or foamed polystyrene. The step of shrinking introduces the distortion in the fiber that increases the LRDF and SRDF. The relatively large values of LRDF and/or SRDF of the novel fibers provide their utility in absorbent products. Shrinking occurs for oriented amorphous polymeric fibers when the fibers are heated above their glass transition temperature. The shrinking occurs either prior to or in the absence of substantial crystallization.

The novel fibers of the invention, preferably, have a surface composition that is hydrophilic which may be inherent due the nature of the material used to make the fibers or may be fabricated by application of surface finishes. Hydrophilic surface finishes provide structures the surfaces of which have large adhesion tension (i.e., that strongly attract) with aqueous liquids and are therefore preferred for applications involving aqueous liquids such as those discussed below for temporary acquisition/distribution structures and permanent storage structures. Preferably, the hydrophilic surface has an adhesion tension with distilled water greater than 25 dynes/cm as measured on a flat surface having the same composition and finish as the surface of the fiber. Some of the finishes/lubricants useful to provide large adhesion tensions to aqueous liquids are described or referenced in U.S. Pat. No. 5,611,981. Surface finishes are well known in the art.

The surface finishes are typically coated on fibers during their manufacture. The coating, i.e. lubricating step, usually occurs just after the molten polymer is extruded through the aperture of a spinnerette and quenched, but it can be applied later as discussed below. The thickness of the coating is much thinner than the cross-section of the fiber and is measured in terms of its percent of the total weight of the fiber. The weight percent of the coating is typically between 0.005 and 2.0 percent of the total weight of the fiber.

Preferably, the fibers have a specific surface force, which is mathematically determined by the following equation:

$$(P\gamma \cos(\theta_a))/d \geq 0.03 \text{ dynes/den}$$

wherein P is the perimeter of the cross-section of the fiber in centimeters (cm); γ is the surface tension of the liquid on the surface in dynes/cm; θ_a is the advancing contact angle of the liquid on a flat surface having the same composition and finish as the surface of the fiber (as specified in U.S. Pat. No. 5,611,981); $\gamma \cos(\theta_a)$ is the adhesion tension of the liquid on the surface of the fiber; and d is the denier of the fiber on which the P was measured. Novel fibers which satisfy this inequality have excellent flow of fluid along their length.

The novel fibers have channels on their surface which may be useful in distributing or storing liquids when the proper surface energetics exist on the surface of the fibers, such as when the fibers satisfy the above equation relating to specific surface forces. The surface energetics determine the adhesion tension between the surface and whatever liquid is in contact with the surface. The larger the adhesion tension, the stronger the force of attraction between the liquid and the surface. The adhesion tension is one factor in the capillary forces acting on the liquid in a channel. Another factor affecting the capillary forces acting on a liquid in a channel is the length of the perimeter of the channel. When the widths of the channels are small, the capillary forces are relatively strong compared to the force of gravity on the

liquid, since the force of gravity on the liquid in a channel is proportional to the area of the channel. Therefore, preferably, the width of the channels is less than 400 microns.

The important advantages of the novel fibers of the present invention are provided (1) by the capillaries defined in the final fiber being less than 400 microns, (2) by the relatively large ratio of the void volume (for storing liquid) to the volume of the material forming the fibers, and (3) by the bulk and rigidity provided by the large LRDF of the fibers. Novel fibers of the present invention may also contain channels which are larger than 400 microns. These features provide the novel fibers with the ability to acquire, transport, and store a relatively large capacity of liquid, and to prevent that liquid from being expelled when the structure is squeezed with moderate pressure. "V"-shaped grooves and/or grooves with wide bases may also be used for these purposes.

The novel fiber of the present invention may also be coated with a superabsorbent polymer (SAP) to increase the ability of the fiber to absorb liquid. Preferably, the novel fibers are coated with up to 35 weight percent of SAP. An additive, such as a surfactant, is preferably mixed with the SAP thereby increasing the hydrophilicity of the mixture relative to the pure SAP. Preferably, the SAP is a copolymer of maleic anhydride and isobutylene. Preferably, the surfactant is a nonionic ethoxylated fatty acid ester. These SAP coated novel fibers are useful in novel absorbent structures which permanently store, whereas the novel fibers without the SAP coating are useful to temporarily store and distribute liquids.

Surprisingly, the initial contact angle of water on a SAP is high. For example, the contact angle of water on the surface of the SAP of Example 6 was visually estimated at about 60 degrees. The contact angle of aqueous liquids on SAP must be reduced in order to have sufficient adhesion tension between the aqueous liquid and the SAP to draw the liquid into and along the channels of the novel fibers. The additive to the SAP lowers the initial contact angle of an aqueous liquid on the SAP surface and enhances transportability of the aqueous liquid in the partially filled grooves.

The novel fibers may be used to address a significant problem with the prior art absorbent products known as gel blocking. For example, gel blocking of SAP occurs when high blend levels of SAP with fluff pulp of greater than 30 percent SAP are used at high densities of greater than 0.10 g/cc to make the currently popular thin diapers. Selected novel fibers of this invention when blended with SAP and fluff pulp will reduce gel blocking.

Novel absorbent structures of the present invention, which function to temporarily acquire and distribute fluids, are made of an assembly of the novel fibers described above. The bulk density of these temporary acquisition/distribution (TA) structures is similar to the bulk density of cellulose fluff pulp, which is preferably less than 0.15 grams per cubic centimeter. The function of temporarily acquiring fluids means that the TA structures may be desorbed by materials which have a greater thermodynamic attraction to the fluids than the TA structures themselves. Examples of desorbing materials in order of increasing thermodynamic attraction include distribution materials, such as those disclosed in U.S. Pat. Nos. 5,200,248; 5,268,229 and 5,611,981 and in co-pending U.S. application titled "Bundles of Fibers Useful for Moving Liquids at High Fluxes and Acquisition/Distribution Structures that Use the Bundles" filed Aug. 15, 1997; fluff pulp; chemically modified fluff pulp; SAP containing materials.

The TA structures preferably have an absorbency of at least 6 grams of water absorbed per gram of material in the structure. The TA structures are resistive to the release of absorbed liquid under pressure. Preferably, the TA structures have less than 50 percent, more preferably less than 30 percent, water released at one pound per square inch (psi) of pressure. The TA structures have a significant reduction in liquid given up under pressure when compared to fluff pulp.

Wet collapse is typically a problem with cellulose fluff pulp, which has a wet collapse of about 25 percent at a bulk density of 0.0393 g/cc. The TA structures, however, have a wet collapse at a bulk density of 0.0393 g/cc of less than 12 percent, more preferably less than 5 percent and still more preferably essentially zero.

In another embodiment of the present invention the novel fibers are utilized in absorbent structures to permanently store fluids along the length of the fibers. The permanent storage (PS) structures comprise the novel fibers coated with SAP and, preferably, with a blend of SAP and surfactant, as described above. The SAP or blend is coated on or partially fills the channels. By using the blend of SAP and surfactant the length of the novel fibers is utilized in the storage of fluids within the channels of the fibers. The PS structures preferably have an absorbency of at least 20 grams of water absorbed per grams of material in the structure, water release at 1 psi of less than 30 percent and a R_{avg} of greater than 2.5 g/sec.

The novel fibers of the present invention and those coated with SAP may be mixed or blended with fluff pulp, chemically treated fluff pulp, SAP or combinations thereof to provide additional structures for permanently storing fluids. In particular blends of the novel fibers of the present invention with fluff pulp provide a permanent storage structure having a wet collapse of less than 5 percent at a density of 0.393 g/cc.

Consumer disposable absorbent products such as diapers, catamenials, adult incontinent devices are improved using the novel fibers and TA and PS structures of the present invention. For example, FIG. 30 shows a plan view of a design for a feminine napkin 300 having a center area 301 designated by a width 302 and a length 303. Several embodiments of the feminine napkin 300 are shown in FIGS. 31–33 utilizing the novel structures of the present invention.

As shown in FIG. 31 the feminine napkin 300 is designed so that a primary impingement zone 310 comprises a portion of a top sheet 311, a TA structure 312 under the top sheet, and a portion of a distribution layer 313 which is just above a portion of back sheet 314. On either side of the impingement zone 310 is a storage core 315. A shielding strip 316 having openings 317 is underneath the storage core and above the distribution layer 313. The distribution layer is above the back sheet 314 and has a length 303, as shown in FIG. 30. The TA structure 312 is protected from communicating with the storage core 315 by shielding strips 318. Optionally, the TA structure may communicate with the core material 315 by adding openings to the shielding strip 318 or by not having any shielding strip. The distribution layer 313 links the impingement zone 310 to the outer areas of the core material 315 through the opening 317 of the shielding strip 316.

The feminine napkin design of FIG. 31 demonstrates the unique features of the novel fibers and in particular the TA structures of the present invention. The top sheet 311 of the feminine napkin 300 is insulted by an aqueous fluid at the impingement zone 310. The TA structure 312 temporarily acquires the aqueous fluid from the top sheet 311. The

aqueous fluid in the TA structure 312 is desorbed by the distribution layer 313 and transferred to the storage core 315. At various points along the length of the storage core 315 designated by the openings 317 of the shielding strip 316, the aqueous fluid is desorbed from the distribution layer to a storage core. This process of fluid management allows for numerous insults to the impingement zone because the TA structures are drained by the storage core, thereby preparing the TA structures for another insult. The process may be repeated until the storage core is saturated. This feminine napkin design allows for complete utilization of the storage core and reduces leakage providing a product that overcomes the problems associated with prior art designs. This same basic design may be applied to diapers and adult incontinent devices. Obviously, the size (volume) of the TA structure will depend on the type of absorbent product that the TA structure is a component of.

In another embodiment, as shown in FIG. 32, the distribution layer 313 is directly underneath the top sheet 311 and has a length 303. The primary impingement zone 310 comprises a portion of the top sheet 311, a portion of the distribution layer 313 underneath the top sheet, and the TA structure 312 under the distribution layer 313 and just above a back sheet 314. On either side of the impingement zone 310 is the storage core 315. The shielding strip 316 is below the distribution layer 313.

In still another embodiment, as shown in FIG. 33, a TA structure 312 is directly underneath a top sheet 311 along the entire length of the top sheet. A distribution layer 313 is underneath the TA structure 312 and above a shielding strip 316. In this embodiment, there is no specified impingement zone. A storage core 315 is below the shielding strip 316 and above a back sheet 314. The top sheet is insulted with an aqueous fluid, which is subsequently acquired by the TA structure. The aqueous fluid is then desorbed from the TA structure and the distribution layer to the storage core.

The top sheet and the shielding strip may be made of any conventional top sheet material such as perforated polyethylene film or a calendar bonded or a spun bonded top sheet made from polypropylene fiber. The top sheet and shielding strip may also be made from other perforated polymer films and fibers. Preferably, the underside of the top sheet has a lower contact angle with aqueous liquids than the top side of the top sheet. In another preferred embodiment the top sheet is made from an apertured film with cut out portions in the aperture walls to provide spontaneous liquid inversion from the frontside of the top sheet to the backside, as disclosed in U.S. application Ser. No. 545,450 filed Oct. 19, 1995.

The distribution layer is preferably fibers like those disclosed in U.S. Pat. Nos. 5,200,248; 5,268,229 and 5,611,981 and in co-pending U.S. application titled "Bundles of Fibers Useful for Moving Liquids at High Fluxes and Acquisition/Distribution Structures that Use the Bundles" filed Aug. 15, 1997. These fibers may be described as having either (a) a Specific Capillary Volume of at least 2.0 cc/g and a Specific Capillary Surface Area of at least 2000 cm²/g or a Slenderness Ratio of at least 9 and at least 30 percent of intra-fiber channels with a capillary channel width of less than 300 microns or (b) a Specific Capillary Volume of less than 2.0 cc/g or a Specific Capillary Surface Area of less than 2000 cm²/g and a Slenderness Ratio of less than 9 or more than 70% of intra-fiber channels with a capillary channel width of greater than 300 microns. Preferably, the fibers described in (b) have a single fiber bulk factor of greater than 4.0. Preferably, the fibers of the distribution layer have a specific surface force, which is mathematically determined by the following equation:

$$(P\gamma \cos(\theta_a))/d \geq 0.03 \text{ dynes/den,}$$

wherein P is the perimeter of the cross-section of the fiber (cm); γ is the surface tension of the liquid on the surface (dynes/cm); θ_a is the advancing contact angle of the liquid on a flat surface having the same composition and finish as the surface of the fiber (as specified in U.S. Pat. No. 5,611,981); $\gamma \cos(\theta_a)$ is the adhesion tension of the liquid on the surface of the fiber; and d is the denier of the fiber on which the P was measured. Novel fibers which satisfy this inequality provide large driving forces to move fluids.

The storage core may be fluff pulp, chemically modified fluff pulp, superabsorbent polymer, the PS structures of the present invention, or combinations thereof. The back sheet is typically made of polyethylene film.

The fibers of the present invention can be made by several different processes. However, the following four sequences of steps are preferable for making the novel fibers.

Process	Sequence of steps
1.	Spin, cut, shrink, lube, package
2.	Spin, shrink, lube, cut, package
3.	Spin, draw, cut, shrink, lube, package
4.	Spin, draw, shrink, lube, cut, package

The spin step means conventionally extruding molten polymer through apertures in a spinnerette forming shaped fibers. When the molten polymer is poly(ethylene terephthalate) the extrusion is at a temperature of about 270 to 300° C. The viscosity of the molten polymer exiting the aperture is preferably between 400 to 1000 poise. The spin step also includes cooling the extruded polymer to form a fiber having an as spun shape, lubricating the fiber, and then transporting the fiber. The preferred transporting (spinning) speeds are between 500 and 3500 meters per minute (m/min). Higher spinning speeds may result in the onset of crystallization in the extruding fiber. Crystallization reduces the ability of the fiber to shrink in the subsequent shrink step and thereby inhibits the formation of the structural distortions. Preferably, the spinning speeds are from 1000 to 1500 m/min and 2500 to 3200 m/min depending on the polymeric material used. Obviously cross-section preservation and amorphous orientation differences within a cross-section are important during the spinning of these fibers. Typically, relatively low melt temperatures, relatively high molecular weight polymers, relatively high quench rates and possible melt surface tension reduction are used to produce the desired shapes and the amorphous orientation differences.

The cut step means conventionally cutting the fibers. The cut lengths of the novel fibers of the present invention are short as compared to the conventional cut lengths of staple PET fibers, typically one and one half inches. The lengths of the cut novel fibers are from 2 to 37 millimeters (mm).

The final lengths of the novel fibers are not necessarily the lengths of the fibers during intermediate steps in the manufacturing process. For example, in the shrink-cut processes (i.e., in the process involving sequential steps of first shrinking the fibers and then cutting the fibers), the fibers are cut to the desired lengths of between 2 and 37 mm. However, in the cut-shrink processes (i.e., in the process involving sequential steps of first cutting the fibers and then shrinking the fibers), the fibers are cut to a longer length than the desired length and then shrunk to the desired length.

The shrink step occurs by subjecting the as spun fiber or a drawn fiber to an environment having a sufficient temperature to effect shrinking of the fiber to a denier of at least

5 percent, preferably 25 percent, greater than the denier prior to shrinking. The shrinking may be done as a modification of a conventional fiber staple process. The shrink step differs depending on whether the process is either shrink-cut or cut-shrink.

In the shrink-cut process, the novel fibers are preferably formed into a tow. The fibers in the tow are then shrunk. The tow is delivered to the shrinking environment at a first speed and removed from the environment at a second speed, which is slower than the first speed. For example, a heated water bath at a temperature of between 70 and 100° C. may be used to shrink the fiber. The fiber is constrained at both ends of the bath by rolls or drums so that the fiber cannot freely rotate. This shrink process is called rotationally constrained shrink. Shrinking the tow in steam or in a hot oven is also possible. The take-up roll that pulls the fiber out of the shrinking region has a lower surface speed than the feed roll delivering the fiber to the heated shrinking region. This difference in delivery and take-up speeds allows the fiber to shrink in the heated shrinking region.

In the cut-shrink process, the cutting of the novel fibers is performed before the shrinking of the fibers. In this process, which is typically called three-dimensional free shrink, the fibers are not constrained during the shrink process. The shrinking may be performed by immersing the cut fibers in an environment suitable to effect shrinking, such as water, hot air, or steam. The cut-shrink process is particularly suitable for high-speed operations on the order of between 2000 and 3500 meters per minute. The spinning, cutting, and shrinking are consecutively and continuously done. For example, a cut shrink process could be designed to provide spinning speeds of about 3000 meters per minute with correspondingly high rates of cutting and with the shrinking done in a high velocity turbulent hot air chamber with a residence time of 1 to about 30 seconds. As the shrunk fiber passes out of the turbulent hot air chamber, the shrunk fiber falls into a bale for packaging and shipment.

In an alternative cut-shrink process, the shrinking step does not occur immediately following the cutting step. For example, the product from the continuous spinning-cutting process can be used to feed a paper making machine. The step of shrinking can take place at the location of the paper making machine. For this alternative example, it is preferred that the packaged material is in the form of rolled sheets.

The lube step means applying a surface finish to the shrunk fiber. Often the surface finish applied in the spinning step is removed during the shrinking step and another application is necessary. Any conventional finish application process may be used. Examples include applying the surface finish using spray booths, lube rolls, metered tips, or even a hot water bath as used for shrinking the fibers. The surface finish is preferably a hydrophilic surface lubricant, which reduces the contact angle and/or increases the adhesion tension of an aqueous liquid with a fiber surface.

The drawing step is optional and may be either a conventional tow or filament drawing step of the type used to form staple fibers, but which does not use heat setting. The main purposes of the drawing step are to reduce the denier per filament of the product, to increase the amorphous orientation differences within a given filament cross-section, and to increase the amorphous orientation of the polymer chains along the fiber axis. Thus, by drawing the fiber before shrinking, the shrinking step will tend to maximize SRDF and/or LRDF. The drawing is performed under substantially amorphous retaining conditions so that the necessary distortions occur when the drawn structure is shrunk. Because of the rotational constrained free shrink, the shrink-cut

processes tend to give relatively high values of SRDF and relatively low values of LRDF compared to the cut-shrink processes.

Referring now to the drawing, in particular FIGS. 1–29, wherein like reference numerals designate identical or corresponding parts throughout the several views, FIG. 1 shows a generally H-shaped orifice or aperture of a spinnerette at a scale of 20 times the actual size of the orifice. The width *W* of the aperture is approximately 84 microns. The aperture extends along **4c+4d** of the “H” for 179 times the width *W* of the aperture. The distance between the arms **4b** and **4c** is 60 *W*. In addition, the base **4e** extends from **2a** to **2b**, which is beyond between the two longest portions of the “H-shape”. The length of the crossbar **4e** of the aperture is 71 *W*. Apertures of the shape shown in FIG. 1 are part of the spinnerette I-1083 that was used to form the novel fibers of Example 1.

FIG. 2 shows photograph **10** including the cross-sections of generally “H-shaped” as-spun fibers formed from the spinnerette I-1083. Photograph **10** at a magnification of 115 (115 \times) shows the general H-shaped fiber cross-section **11** which includes four arms such as the arms **12a**, a cross-bar **12b** connecting to proximal ends of each of the arms, and two projections **12c**. The arms **12a** of the cross-section **11** are approximately twice as long as the cross-bar **12b** and have a length to width ratio of between about 8 and about 12. The channels **13** and **14** are approximately equivalent in width, depth, and area.

FIG. 3 shows seven cross-sections of the novel fibers, each having a distorted “H” shape. Frame **30** delimits the seven cross-sections, which were each taken from photographs at 111 \times . Cross-section **33** is delimited by a polyhedron **31**. The polyhedron **31** includes the segments **32a**, **32b**, **33c**, and **32d**, which define the polyhedron **31**. Each of the segments **32a–32d** is tangent to two points on the surface of the cross-section **33**. Adjacent segments form an interior angle interior to the delimited area of the polyhedron **31**, that is less than 180°. The segments **32b** and **32c** meet at the point **34**. The segments **32c** and **32d** meet at the point of **35**. FIG. 3 shows that the cross-sections of the novel fibers vary significantly due to the shrinking process leading to the short range distortion factor.

FIG. 4A shows a photograph **40** at 7 \times of the novel fibers of **41a–41f** of Example 1. There are two rows of numbers in FIG. 4A. The upper row of numbers, including 7.74, 7.45, 7.49, 7.32, 8.17, and 7.76, are the measured values of the length along the backbone of the fibers **41a–41f**. The lower row of numbers, including 6.8, 6.7, 6.8, 6.6, 7.0, and 6.9, are the measured values for the diameter of a circle circumscribing each of the fiber **41a–41f**. All of the lengths and diameters are in millimeters and are the actual values from the unmagnified novel fibers.

FIG. 4B shows the photograph **45** at 40 \times of the novel fibers of Example 1. Polymeric structure **46** includes the arm or wall **47** and the base **48**. The azimuthal location of the arm **47** varies along the length of the backbone. The azimuthal angle of the arm **47** changes by 360 degrees along the length of the backbone **48** over a length of the backbone of about 750 microns.

FIG. 5 shows a design drawing of an aperture **50** of the spinnerette I-1042 used in Examples 2 and 19. Aperture **50** includes arms **51a**, **51b**, **51c**, and **51d**, a cross-bar **52**, and projections **53a**, **53b**. The width *W* of the aperture **50** is 0.100 mm. Each of the arms **51a–51d** has a length of 50 *W*. At the free end of **51a–51d**, there is a circular diameter of 1.3 *W*. Each of the projections **53a**, **53b** has a length of 5 *W*. The cross-bar **52** (including the projections **53a** and **53b**) is 60 *W* long.

FIG. 6 shows a frame **60** delimiting portions of seven photographs at 285 \times each showing a cross-section of a novel fiber for Example 2. FIG. 6 also shows the cross-section **61** having an arm **62** and a cross-bar **63**. The length of the arm **62** is between 30 and 40 microns. The width of the arm **62** is between 5 and 10 microns. The length of the cross-bar **63** is between 25 and 35 microns. The length to width ratio of the arm **62** is approximately 5.

FIG. 7A is a photograph **70** at 80 \times showing the novel fiber **71** of Example 2. The fiber **71** shows oscillations in the azimuthal location of the walls or arms **72** have a periodicity length **73** which is about 112 microns. The backbone **74** of the fiber **71** is relatively straight over the 112 micron length scale of the oscillations in the azimuthal location of the wall or arm **72**.

FIG. 7B is a photograph **78** showing novel fibers of Example 2 at 36 \times .

FIG. 7C is a photograph **79** at 7 \times showing three novel fibers of Example 2. The numbers 9.79, 7.18, and 8.0 in FIG. 7C corresponds to the length along the backbone of the fibers shown in the left, center, and right sides of FIG. 7C, respectively. The number 7.7, 6.0, and 6.0 shown in the lower half of FIG. 7C correspond to the diameters of a circle circumscribing the fibers shown in the left, center, and right sides of FIG. 7C, respectively. The fiber **75** has the ends **76** and **77**. All of the lengths and diameters are in millimeters and are the actual values from the unmagnified novel fibers.

FIG. 8 is a photocopy of portions of six photographs at 285 \times , each showing cross-sections of the novel fibers of Example 3. FIG. 8 includes the border **80** delimiting the views of the six cross-sections **81**, **82**, **83**, **84**, **85**, and **86**. The lengths of the arms shown in FIG. 8 vary from about 24 microns to about 50 microns. The widths of the arms shown in FIG. 8 vary from about 7 to about 12 microns. The lengths of the cross-bars connecting arms on opposite sides of the distorted H-shaped cross-sections are between about 14 and about 25 microns.

FIG. 9A is a photograph **90** at 7 \times showing the novel fibers **93a–93d** of Example 3. FIG. 9A shows the numbers 7.72 and 6.50 corresponding to structure **93a**, the numbers 8.08 and 6.70 corresponding to structure **93b**, the numbers 8.20 and 7.10 corresponding to structure **93c**, and numbers 8.56 and 6.80 corresponding to the structure **93d**. The upper and lower numbers in FIG. 9A that correspond to each structure are the length along the backbone and the diameter of the circle circumscribing the structure, respectively. All of the lengths and diameters are in millimeters and are the actual values from the unmagnified novel fibers.

FIG. 9B is a photograph **94** at 40 \times showing the novel fibers **95** of Example 3.

FIG. 10 is a photograph **100** at 7 \times of novel fibers of Example 4. FIG. 10 shows the novel fibers **103** having the ends **101** and **102**. FIG. 10 also shows the novel fibers **104**. The novel fibers **103** and **104** have the length along their backbones of 16.05 and 17.35 respectively, and diameters of circumscribing circles of 9.6 and 9.3 respectively. All of the lengths and diameters are in millimeters and are the actual values from the unmagnified novel fibers.

FIG. 11 shows a frame **110** framing a design drawing of an aperture **111** of a spinnerette. The aperture **111** includes the ends **112**, **113**, the straight extending portions **115**, **116**, and the projecting portions **114a–114e** of the circular section **114**. The ends **112**, **113** are circular in shape with a diameter of 1.3 *W*. The aperture **111** includes the inner surface **118** of the extending portions **115**, **116** and the circular section **114**, which defines the channel **117**. The width *W* of the aperture is 0.100 mm. The length of the extending portions **115**, **116**

are each 28.75 W. The angles between a normal to the extending portion **116** and the projection **114e** is 30°. The angles between each adjacent ones of the projecting **114a–114e** is 30°. A radius of curvature of the circular section **114** is 18.4 W.

FIG. **12** shows a photograph **120** at 464× of fibers in an as spun state, which were spun from a spinnerette having the aperture shown in FIG. **11**. The cross-section **120a** shown in FIG. **12** has the ends **121**, **122** from which extend the extending portions **124**, **125**. The cross-section **120a** also includes the projections **123a–123e** and has the inner surface **127** defining the channel **126**. The extending portions **124**, **125**, are approximately 75 microns long. The width W of the channel **126** at its mouth is approximately 55 microns. The projecting portions **123a–123e** project between 5 and 10 microns. A width of the extending portions **124**, **125** at their mid-sections is between 5 and 10 microns.

FIG. **13** shows border **130** delimiting portions of four optical photographs at 285×, each show a cross-section of a novel fiber of Example 12. FIG. **13** shows the cross-sections **131**, **132**, **133**, and **134**. The cross-section **132** actually contains cross-section **135**, which is in registration with cross-section **132**. Cross-section **131** shows a channel that is wider than the channel of the pre-shrunk fiber shown in FIG. **12**. Cross-section **134** shows a channel that is much narrower than the channel of the pre-shrunk fiber in FIG. **12**. The cross-section **133** is shown delimited by a polyhedron including segments joining at points **137** and **138**. FIG. **13** shows that the morphology of the channel shown in FIG. **12** is highly distorted after the shrink process.

FIG. **14** is a photograph **140** at 7× of five novel fibers of Example 12. The novel fibers are **141a–141e**. The lengths along the backbone of the five fibers are 7.71, 6.93, 7.18, 7.03, and 7.10 millimeters, respectively. The lengths of the circumscribing circles of fibers **141a–141e** are 6.9, 6.2, 6.3, 6.4, and 6.1 millimeters, respectively, all as shown in FIG. **14**. All of the lengths and diameters are in millimeters and are the actual values from the unmagnified novel fibers.

FIG. **15** shows a photograph **150** at 7× of novel fibers of Example 13. The novel fibers **151a–151e** have lengths along their backbones of 4.87, 5.96, 5.55, 5.91, and 6.13 millimeters, respectively, and diameters of circumscribing circles of 3.8, 4.1, 4.8, 3.8, and 4.5, respectively, all as shown in FIG. **15**. All of the lengths and diameters are in millimeters and are the actual values from the unmagnified novel fibers.

FIG. **16** is a design drawing schematic of an aperture **160** of the spinnerette I-1004. The shape of the aperture **160** is called a “4DG” aperture shape. The numbers along the segments in FIG. **16** indicate the relative length of each segment relative to the width W of the aperture. The width W of the aperture is 0.100 mm. The angles between segments in FIG. **16** are actually angles, not merely illustrative. The free end **161** of each segment is a circular hole with a diameter of 1.5 W.

FIG. **17** shows a photograph **170** at 464× of cross-sections of as spun fibers of Example 14 having a cross-sectional shape derived from extrusion from the spinnerette I-1004, the apertures of which have the 4DG shape. The shape of the cross-section shown in FIG. **17** is called the 4DG cross-section shape. The photograph **170** shows the fiber cross-section **171**. The cross-section **171** includes walls or arms **172a–172h** and a backbone or spine **173** that defines channels **174a–174h**. The length of the backbone or spine **173** is about 110 microns. The lengths of the walls or arms forming the channels range from about 15 to about 45 microns. The widths of the channels at their mouth range from between

about 20 and about 55 microns. The two channels at the end of the backbone or spine **173** are “V” shaped. The remaining channels are defined by at least two walls and a base. The thickness of each of the arms or walls and the spine are between about 6 and about 10 microns. The two widest channels, channels **174a** and **174e** are defined by, in addition to the two walls and base, segments at an angle of about 45 degrees relative to the base and that the walls that connect the base to the walls. A better view of the segments connecting the base to the walls of the widest channels appears in the cross-section **175**.

FIG. **18** is a photograph **180** at 7× of the novel fibers **181a**, **181b**, and **181c** of Example 14. The length along the backbone or spine for structures **181a–181c** is 7.12, 7.10, and 7.56 respectively, and the diameter of the circumscribing circle for structures **181a–181c** is 6.4, 6.5, and 6.8, respectively, all as shown in photograph **180**. All of the lengths and diameters are in millimeters and are the actual values from the unmagnified novel fibers.

FIG. **19A** includes a border **190** delimiting portions of three photographs at 285×, each showing a cross-section of a novel fiber of **191a**, **191b**, and **191c** of Example 15. Cross-section **191b** is enclosed by line segments forming a polyhedron. Two of the lines segments of the polyhedron meet at the point **192** and two of the line segments of the polyhedron meet at the point **193**. Each line segment is tangent to two points on the surface of the cross-section. Adjacent line segments form an angle interior to the polyhedron of less than 180 degrees. The cross-section **191a** is identified by the number 36. The cross-section **191b** is identified by the number 46. The cross-section **191c** is identified by the number 2.

FIG. **19B** includes a boarder **195** containing portions of two photographs at 285×, each showing one of the cross-sections **196a** and **196b** of the novel fibers of Example 15. The cross-section **196a** is identified by the number 35. The cross-section **196b** is identified by the number 12.

FIG. **20** shows a photograph **200** at 7× of the novel fibers **201a–201d** of Example 15. The length along the backbone or spine of structures **201a–201d** is 4.40, 4.46, 4.41, and 3.69 mm respectively. The diameter of the circle circumscribing the structures **201a–201d** is 2.9, 3.0, 2.6, and 2.2, respectively, all as shown in photograph **200**. All of the lengths and diameters are in millimeters and are the actual values from the unmagnified novel fibers.

FIG. **21A** shows a schematic in plan view of an Y shaped aperture design **210** for the apertures of the spinnerette **215** (see FIG. **21B**) identified as I-1195. The aperture **210** includes arms **211a**, **211b**, and **211c**. The arms **211a** and **211c** define an angle of 110 degrees between them. The arms **211a** and **211b** define an angle of 125 degrees between them. The arms **211b** and **211c** define an angle of 125 degrees between them. The width W of the aperture is 0.067 mm. The lengths of each of the arms of the aperture **210** are 150 W.

FIG. **21B** is a schematic plan view of the spinnerette **215** identified as I-1195 showing the ten Y shaped apertures **210**. The face **218** of the spinnerette includes the Y shaped aperture **217** and the bores **216** in spinnerette **215**. Delimiting the face of the spinnerette in the plan view in FIG. **21b** is the flange surface **219** of the spinnerette **215**.

FIG. **22** shows the photograph **220** at 115× showing the cross-section **221** of an as spun fiber of Example 20. The cross-section **221** includes the arms **222**, **223**, and **224**, which have distal tips **225**, **226**, and **227**. The arms **224** and **222** meet at the vertex **228** and define an angle of greater than 120 degrees. The arms **222** and **223** meet at the vertex

229 and define an angle of greater than 120 degrees. The arms **223** and **224** meet at the vertex **230** and define an angle of less than 120 degrees. The length of the arms range between about 216 and about 310 microns. The width of the arms at the mid section range between about 15 and about 20 microns. The arms **223** and **224** have a slight curvature concave towards one another. However, the alignment of each arm does not vary by more than 60 degrees. That is, a line that is best aligned along any 100 micron long section of either of the arms **223**, **224** defines an angle of less than 60 degrees with any other line aligned along another 100 micron long section of the same arm.

FIG. **23** shows a border **235** delimiting portions of a four photographs at 111x, each showing one of the novel fibers **236**, **237**, **238**, and **239** of Example 20. Cross-section **236** shows three arms **236a**, **236b**, and **236c**. The angle defined by the portions of the arm **236a** and **236c** where those arms join another is approximately 180 degrees. The remaining two angles defined by the portions of the arms **236a**, **236b**, and **236c** where those arms join are each less than about 90 degrees. The lines aligned with the arm **236a** and **236c** along 100 micron sections thereof vary by more than 60 degrees. Cross-section **237** includes arms that define the vertices **240**, **241**, **242**. The arms of the vertex **238** define an angle of about 180 degrees. The arms of the vertices **239**, **240** define angles less than about 120 degrees. Cross-section **238** is shown enclosed in a polyhedron. The lengths of the arms of the cross-sections shown in border **235** are between about 210 and 350 microns. The widths of the arms of the cross-section shown in border **235** at the mid sections of the arms vary between about 8 and about 16 microns.

FIG. **24** shows a photograph **245** at 7x of the novel fibers **246** and **247** of Example 20. The length along the backbone or spine of structures **246**, **247**, are 14.92 and 13.90, respectively. The diameters of the circumscribing circles of structures **246** and **247** are 7.7 and 7.8 respectively. All of the lengths and diameters are in millimeters and are the actual values from the unmagnified novel fibers.

FIG. **25** is a schematic **250** of a design drawing of an aperture in the spinnerette identified as I-1198 used to make the novel fibers of Example 21. The aperture **250** includes the two short arms **253** and **254** and the two long arms **251** and **252**. The width *W* of the aperture is 0.067 mm. The length of arm **253** is 40 *W*. The length of arm **254** is 80 *W*. The length of the arm **251** is 196 *W*. The length of the arm **252** is 183 *W*. The arms radiate from a common point at 90 degrees relative to one another. The two short arms form an angle of 90 degrees and the two long arms form an angle of 90 degrees.

FIG. **26** is a photocopy of portions of six photographs at 115x, each showing one of the cross-sections **261a**–**261f** of a novel fibers of Example 21. Each cross-section contains two long arms and two short arms. The lengths of the short arms vary from between about 35 and about 70 microns. The lengths of the long arms vary from between about 130 and 340 microns. The width of the long arms at their mid sections vary between about 8 and about 16 microns. The two short arms are adjacent to one another with no long arm intervening between them. All four arms extend from a common point in the cross-sections, which means that all four arms extend from a common backbone or axis along the length of the structure.

FIG. **27** shows a photograph **270** at 7x of novel fibers **270a**, **270b**, and **271c** of Example 21. The lengths along the backbone or spine of the structures **271a**–**271c** are 8.68, 9.33, and 7.35 mm, respectively. The diameter of the circumscribing circle for structures **271a**–**271c** are 7.1, 6.7, and

6.0 mm, respectively. All of the lengths and diameters are in millimeters and are the actual values from the unmagnified novel fibers.

FIG. **27B** shows a photograph at **272** at 40x of the novel fibers **273a**, **273b**, and **273c** of Example 21. FIG. **27B** shows the length **274** of 200 microns over which the azimuthal orientation of the wall **275** appears to undergo one complete sinusoidal oscillation in azimuthal position.

FIGS. **28A**–**B** illustrate the definition of the single fiber bulk factor which is the cross-sectional area of the channels divided by the cross-sectional area of the fiber. FIG. **28A** shows a fiber cross-section **280** having a width *W* and arms **282A**, **282B**, and **282C** having distal tips **283A**, **283B**, and **283C**. The arms **282A**, **282B**, and **282C** define the cross-sectional channel areas **281A**, **281B**, and **281C**. The cross-sectional channel areas **281A**, **281B**, and **281C** are defined by the straight line segments tangent to the distal tips of the arms and the surfaces of the arms. A determination, in arbitrary units, of the cross-section area of the channels provides an area of **225**. A determination of the cross-sectional area of the fiber in the cross-section **280** provides an area of 60. Therefore, the single fiber bulk factor for the cross-section **280** is 225/60=3.8. FIG. **28B** shows the fiber cross-section **290** and the cross-sectional area of the channel **291** in hashing. Determination, in arbitrary units, of the area of the cross-section of the channels **291** and the area of the cross-section **290** of the fiber provides **225** and **44**, respectively, in arbitrary units. Therefore, the single fiber bulk factor for FIG. **28B** is 5.1.

FIG. **29** is a schematic cross-section of a fiber (solid line) enclosed by line segments AB, BC, CD, and DA (dashed lines) between the points A, B, C, and D. The line segments between the points a, b, c, and d enclose the channel regions A1, A2, A3, and A4. The arms **291** and **294** meet at an end of base **295**. The arms **292** and **293** meet at another end of base **295**.

EXAMPLES

Example 1

Example 1 discloses the preparation of novel fibers that in the as spun state have H-shaped fiber cross-sections. The novel fibers were made using the “spin-shrink-lube-cut” process.

Poly(ethylene terephthalate) (PET) polymer having an inherent viscosity (IV) of 0.70 with 0.2% TiO₂ was used. IV was measured at 25° C. at a polymer concentration of 0.50 g/100 milliliters (mL) in a mixture of 60 weight percent (wt %) phenol and 40 wt % tetrachloroethane. The polymer was dried to a moisture level of less than or equal to 0.003 wt % in a Patterson Conaform dryer at 120° C. for a period of 8 hours. The polymer was extruded at 282° C. through an Egan extruder 1.5" (38.1 mm) diameter, with a length to diameter ratio of 28:1. The fiber was extruded through the 38 orifice spinnerette I-1083, wherein each aperture had the generally “H” shape shown in FIG. **1**. The quench air system had a crossflow configuration. The quench air velocity was about 103 ft/minute. A spinning lubricant was applied via ceramic kiss roll. The lubricant level on the fiber was about 0.50% by weight. Fibers of 23.9 dpf (26.6 dtex) as spun were wound at 2200 meters per minute (m/min) on a Barmag SW4SL winder. FIG. **2** shows cross-sections of the as-spun fibers of Example 1. The as-spun fiber had a shape factor of 4.02.

Thirty packages of fibers were made on the Barmag winder. Doff time for each package was 5 minutes. The undrawn fibers were creeled (all 30 packages) and dried on

a hot-air dryer oven at 200° C. for 5 minutes. The fibers were shrunk in the dryer. A spinning lubricant was sprayed in an amount of 0.8 wt % on the tow after the tow had been dried. Then, the fibers were cut to ¼ inch staple lengths. The resulting fibers were very distorted and were representative of novel fibers of the present invention.

The composition of spinning lubricant was a 10 wt % solids water dispersion of the following composition: 98 wt % solids polyethylene glycol (20) sorbitan monolaurate and 2 wt % solids 4-cetyl, 4-ethyl morpholinium ethosulfate.

FIG. 3 shows seven cross section of the novel fibers at different positions along the length of the fibers. As apparent from FIG. 3, the cross-sections are highly variable. The shrinking step distorted the cross-section. The distortion is characterized by (1) a short-range distortion factor (SRDF) and (2) a long-range distortion factor (LRDF). These distortion factors are measured as per procedure described hereinbelow.

FIGS. 4A and 4B show photographs of the shrunk and cut fibers at 7× and 40× magnification. The structural properties for the novel fibers of FIGS. 4A and 4B were a dpf of 33 (36.7 dtex); staple cut length=¼" (6.4 mm); average length along the backbone contour $L_0=8.2$ mm; average diameter of circumscribing circle $L_1=6.9$ mm; SFBF=2.7; SRDF=26; and LRDF=0.15.

The absorbency characteristics for the novel fibers of Example 1 at a fiber bulk density of 0.0393 g/cc were as follows: absorbency of 10.9 g water/g fiber; wet collapse of 0%; water release at a pressure of 1 psi of 26.8%; R_1 (defined as the initial rate of water absorption upon the first insult by the liquid in grams per second) of 21.7 g/sec; and R_{avg} (defined as the average rate of initial water absorption during 2nd, 3rd, 4th, and 5th liquid insults, $(R_2+R_3+R_4+R_5)/4$) of 1.7 g/sec. Details of measuring these absorbency characteristics are discussed below.

FIG. 4A shows six individual fibers. The numbers in the upper row were the measured values for the lengths L_0 along the backbone of the fibers to which they are adjacent. The numbers in the lower portion of the figure were the diameter L_1 of circle circumscribing the respective fiber. For example, the filament on the extreme left hand side of FIG. 4A had $L_0=7.74$; $L_1=6.8$; and therefore the LRDF= $(L_0-L_1)/L_0=(7.74-6.8)/7.74=0.12$. Likewise, the LRDF, for 50 fibers were measured and averaged to obtain the average LRDF for cut fibers of Example 1 of 0.15.

FIG. 3 shows cross-sections of the materials of Example 1 at 111×. Each cross-section photograph was circumscribed by a polygon as per procedure described for SRDF. Material Area, M_{area} , is the cross-sectional area of the polymer structure. For the cross-section identified by number 2 in FIG. 3, $M_{area}=4346\mu^2$. Channel area (C_{area}) is the area enclosed between the sides of the polygon and the polymer structure. For cross-section number 2, $C_{area}=8450\mu^2$. The ratio C_{area}/M_{area} for cross-section number 2 is 1.94. The C_{area}/M_{area} ratio was calculated for 50 cross-sections, and their average (X_{av}) and standard deviation σ determined for the 50 measurements. The SRDF is defined to be the percent of the coefficient of variations of the channels' cross-sectional area to the material's cross-sectional area, or $SRDF=(\sigma/X_{av})*100$. For the material of Example 1, SRDF is 26.

Example 2

Example 2 discloses the preparation of novel fibers having H-shaped fiber cross-section in the as spun state. These novel fibers were made via the "spin-draw-shrink-lube-cut" process.

The extrusion system was the same as in Example 1. The spinnerette identified as I-1042 having 46 apertures with the shape and dimensions as shown for FIG. 5 was used. PET having an IV of 0.76 was used. The extrusion temperature was 286° C. Quench air flow velocity was 68 ft/min which corresponded to a ΔP of 0.30 inches of water. The spinning lubricant was the same as in Example 1. The take-up speed was 1800 m/min. The as-spun fiber had a "H" cross-section shape and the dpf was 11.2. Forty packages of 7-minute doff time were made. The shape factor of the as-spun fiber was 2.96. The rest of the fiber extrusion process was the same as described for Example 1.

As-spun fibers were further processed on a tow line. Forty ends were in a creel. The tow was drawn in a water bath at 70° C. at a draw ratio of 1.84×. The tow was fed to the water bath at 24.5 m/min and the exit draw roll speed was 45 m/min. A de-watering air jet at 20 psi was used to remove excess water from the tow bundle. The tow was further processed to provide rotationally constrained shrink through a hot-air oven at a temperature of 196° C. for 3 minutes. The lubricant of Example 1 containing 80 wt % solids and 20 wt % water was sprayed after the dryer. The fibers were cut to ¼" staple length via a model 66 cutter. FIG. 6 shows the cross-sections of these fibers. Note the variations in the cross-sections shown in FIG. 6.

FIGS. 7a, b, and c show optical photographs at 80×, 36×, and 7× magnification for the shrunk cut fibers for Example 2. The characterization of these material was as follows: dpf=9.8 (10.9 dtex); Cut Staple Length=¼" (6.4 mm); Avg. Length along the backbone, $L_0=8.3$ mm; Avg. diameter of circumscribing circle, $L_1=6.7$ mm; SFBF=2.0; SRDF=27; and LRDF=0.18.

Absorbency characteristics for Example 2 at 0.0393 g/cc density were as follows: Absorbency=15.2 g H₂O/g; Wet Collapse (%)=1.7%; Water release at 1 psi=30.4%; $R_1=25.1$ g/sec; and $R_{avg}=0.7$ g/sec.

Example 3

Example 3 discloses the preparation of novel fibers having H-shaped fiber cross-section in the as spun state. These materials were made via the "spin-shrink-lubecut" process as in Example 1.

The extrusion system was the same as used in Example 1. The polymer used in this Example was PET of 0.76 IV, spinnerette used was H-shaped I-1083 with 38 orifices. Extrusion temperature was 282° C. Quench air flow corresponded to 0.70 inch water pressure drop (air velocity of 103 ft/minute). Spinning lubricant was the same as Example 1. Take-up speed was 2200 m/min. As-spun dpf=24.8. Total package denier=944. Shape factor of as-spun fiber=3.28. The rest of the fiber extrusion process was same as described in Example 1. Thirty-nine packages were spun with a doff time of 7 minutes.

As-spun fibers were further processed on a tow line. The fibers were shrunk at 195° C. for 5 minutes in the dryer-oven and cut to ¼" length.

These novel fibers had a dpf of 55. FIG. 8 shows the cross-section of the novel fibers. FIG. 9 shows the optical photograph of the novel fibers at 7× and 40× magnification.

The characteristics of novel fibers were as follows: dpf=55 (61.1 dtex); Cut Staple Length=¼" (6.4 mm); Avg. length along the backbone, $L_0=8.7$ mm; Avg. diameter of circumscribing circle, $L_1=6.8$ mm; SFBF=1.6; SRDF=32; and LRDF=0.20.

Absorbency characteristics at 0.0393 g/cc density were as follows: Absorbency=7.1 g H₂O/fiber; Wet Collapse=

21

11.1%; Water release at 1 psi=26.4%; R₁=15.5 g/sec; and R_{avg}=1.1 g/sec.

Example 4

Example 4 shows the novel fibers of present invention cut to 1/2" staple length. These novel fibers are made as in Example 3, and were cut to 1/2" staple length instead of 1/4" staple length of Example 3. FIG. 10 shows these novel fibers at 7x. Physical characteristics of novel fibers were as follows: dpf=55 (61.1 dtex); Cut Staple Length=1/2 inch; Avg. length along the backbone, L₀=16.3 mm; Avg. diameter of circumscribing circle, L₁=11.9 mm; SFBF=1.9; SRDF=29; and LRDF=0.26.

Absorbency characteristics of the novel fibers at 0.0393 g/cc density were as follows: Absorbency=6.6 g H₂O/g material; Wet collapse=0%; Water release at 1 psi=26.9%; R₁=12.9; and R_{avg}=0.9.

Example 5 (comparative)

Example 5 shows the absorbency characteristics of fluff pulp. Fluff pulp suffers from high wet collapse (25%) and high water release under pressure (58.3% at 1 psi). Absorbency characteristics of fluff pulp at 0.0393 g/cc density were as follows: Absorbency=19.6 g water/g fiber; Wet Collapse (%)=25%; Water release at 1 psi=58.3%; R₁ initial rate, 1st insult=25.2 g/sec; and R_{avg}=2.5 g/sec.

Example 6

Example 6 fibers were made using the novel fibers of Example 1 and a superabsorbent polymer (SAP) precursor solution available from Camelot Superabsorbents, Ltd., of Calgary, Alberta, Canada. U.S. Pat. No. 5,151,465 discloses uncured polymer compositions that can be made into fibers using conventional fiber-forming processes and cured to produce fibers capable of absorbing at least 60 times their weight of 0.9% sodium chloride solution. The SAP precursor was identified as Fibersorb SA 7200, CTS-HMW. Based on Camelot's MSDS and patents assigned to Camelot, the composition of SAP precursor solution was approximately as follows 74.5 wt % water, 19.5 wt % Trade Secret 4802-01, 5.0 wt % Sodium Hydroxide, 0.6 wt % Glycerol, and 0.4 wt % Trade Secret 4803-02.

The composition of Trade Secret 4803-01 is believed to be a copolymer of maleic anhydride and isobutylene of equal mole ratios of the two noted monomers. Typical molecular weight of the copolymer is in the range of 200,000 to 300,000. The composition of Trade Secret 4803-02 is not known, but likely includes a second cross-linking agent which is the function of glycerol.

Fifty grams of starting material shrunk to 33 dpf was sprayed with 105 g of 5% SAP precursor solution obtained from Camelot. The starting material was sprayed with the SAP solution and was dried in an oven at 120° C. for 60 minutes. The dried sample was further cured at 195° C. for 16 minutes. The cured sample was fluffed in a blender and stored for absorbency testing. This process of making novel fibers enables coating the grooves of the fiber with a superabsorbent polymer.

Coating the grooves with SAP helps in permanent storage and distribution of bodily liquids in absorbent products utilizing these novel fibers. The novel fibers had theoretically 5.25 g of SAP coated per 50 grams of the starting fiber or 9.5% of SAP coated on final fiber. The results of the absorbency testing at 0.0393 g/cc density for the final fiber were as follows: Absorbency=20.9 g H₂O/g; Wet Collapse

22

(%)=0%; Water release at 1 psi=29.1%; R₁=5.2 g/sec; and R_{avg}=5.9 g/sec.

Example 7

The starting material for Example 7 was the novel fibers of Example 1. 210 grams of 5% SAP precursor solution from Camelot was sprayed onto 50 grams of starting material. The sprayed sample was dried in an oven at 120° C. for 80 minutes and further cured at 195° C. for 16 minutes. The resulting novel fibers theoretically were 16.67% SAP coated on 83.33% base material. The novel fibers were fluffed in a blender and stored in zip-lock plastic bags for subsequent absorbency testing.

The results of the absorbency testing at 0.0393 g/cc density were as follows: Absorbency=26.1 g H₂O/g; Wet Collapse (%)=0%; Water release at 1 psi=20.7%; R₁=4.2 g/sec; and R_{avg}=4.5 g/sec.

Example 8

The novel fibers of Example 1 were used as the starting material. 535 grams of 5% SAP precursor solution was sprayed onto 50 grams starting material. The sprayed sample was dried at 120° C. for 165 minutes and cured at 195° C. for 16 minutes. The resulting novel fibers theoretically had 33.3% SAP and 66.7% by weight starting material. The novel fibers were fluffed in a blender and stored in plastic zip-lock bags.

Water absorbency was significantly enhanced as one increases the amount of SAP. The results of the absorbency testing at 0.0393 g/cc density were as follows: Absorbency=41.1 g H₂O/g; Wet Collapse (%)=0%; Water release at 1 psi=8.1%; R₁=5.2 g/sec; and R_{avg}=3.0 g/sec.

Example 9

Blends of fluff pulp and the novel fibers of Example 1 (33 dpf, H-cross-section, 1/4" cut) were made in a blender and the resulting materials were tested for absorbency behavior at a density of 0.0393 g/cc. Following blends were tested:

Blend Composition					
Fluff Pulp (%)	Materials of Example 1 (%)	Wet Collapse (%)	Absorbency (g H ₂ O/g Blend)	R1 Initial Rate Upon 1 st Insult g/sec.	Water Released at 1 psi Load (%)
100	0	25.0	19.6	25.2	58.3
80	20	20.1	20.6	27.5	52.0
60	40	14.9	19.6	26.3	48.4
40	60	10.7	18.8	26.3	39.0
20	80	5.9	15.6	25.5	28.6
0	100	0.0	10.9	21.7	26.8

The wet collapse of blended materials reduces significantly when compared with the wet collapse of fluff pulp. Also, percent water release at 1 psi decreases significantly with increasing levels of starting materials.

Example 10

The fibers of Example 10 were prepared using a spin-shrink-lube process instead of the shrink-cut process of Example 1. Using as-spun fibers of Example 1 for the starting material, an as-spun sample of 23.3 dpf, H-shaped cross-section was made at 3000 m/min spin speed. Quench air flow of 112 ft/min air velocity corresponded to a ΔP of

0.80 inches water was made from the I-1083 spinnerets. The rest of the parameters were the same as that for Example 1. The as-spun fiber was cut into ½", 1", 1½" and 2" staple fiber lengths (about 10 g at each length). These cut samples were shrunk in an oven at 170° C. for 5 minutes and sprayed with about 1% of a spinning lubricant. The lubricant was a 10 wt % solids water dispersion of the following components: 10 wt % solution of poly[polyethylene glycol (1400) terephthalate], 44.1 wt % solids polyethylene glycol (400) monolaurate (oxyethylene fatty acid ester), 44.1 wt % solids polyethylene glycol (600) monolaurate (oxyethylene fatty acid ester), and 1.8 wt % solids 4-cetyl, 4-ethyl morpholinium ethosulfate (alkyl quaternary ammonium salt of inorganic ester).

The shrinkage was about 50%. The results of the absorbency test for spin-cut-shrink-lube process fibers of Example 10 are shown below:

As-Spun Fiber Cut Length	% Wet Collapse	Absorbency g/H ₂ O/g Fiber
½"	2.4	13.2
1"	0	11.2
1½"	0	12.2
2"	0	13.1

Example 11

The fibers of Example 11 were prepared using a spin-draw-cut-shrink-lube process. 7 dpf fibers having 4DG-shape cross-section were spun and drafted on a tow line. The as-spun fibers had a shape factor of 2.9. The fibers were subjected to a two-stage draw with the first stage being in a water bath at 70° C. having a draw ratio of 1.75x and the second stage being in a steam chest at 146° C. having a draw ratio of 1.3x. The overall draw ratio was about 2.25x. The drawn fiber was then cut to ¼" staple length and subsequently heat-shrunk in an oven at 200° C. for 5 minutes.

The physical characteristics of the novel fibers were as follows: dpf=6.5; SFBF=0.5; SRDF=26; LRDF=0.32; L₀=11 mm; and L₁=7.4 mm. The results of the absorbency testing at 0.0536 g/cc density were as follows: Absorbency=16.8 g H₂O/g; Wet Collapse (%)=0%; Water release at 1 psi=44%; R₁=9.2 g/sec;

Example 12

U-shaped fibers were extruded through the Egan extruder of Example 1. The following spinning parameters were used. The spinnerette used in Example 12 was I-1127 having 16 orifices, each having the dimension shown in FIG. 11. PET having a 0.70 IV and 0.2 wt % TiO₂ was extruded. Quench air velocity was 114 ft/min. Extrusion temperature was 282° C. The lubricant used was the same as Example 1. Take-up speed was 3000 m/min. The as-spun fiber had a dpf of 19.9 and a shape factor of 3.58. The as-spun fiber was heat shrunk in a dryer oven at 180° C. for 5 minutes and then cut to ¼" staple length. FIG. 12 shows the fiber cross-section of the as-spun fiber. FIG. 13 shows the cross-section of the resulting novel fibers of the present invention. FIG. 14 shows a photocopy of a photomicrograph of these novel fibers. The ¼"-cut fibers were tested for absorbency behavior at 0.0393 g/cc density with the following results: Absorbency=12.8 g H₂O/g; Water release at 1 psi=60.5%; R₁=20.7 g/sec; and R_{avg}=1.3 g/sec. The structural properties of these fibers are as follows: dpf=28; SFBF=0.8; SRDF=66; LRDF=0.11; L₀=7.3 mm; and L₁=6.5 mm.

Example 13

In Example 13, the novel fibers obtained from Example 12 cut to the ¼" staple size were further shrunk in hot water at 90° C. for 1 minute and dried in an oven at 120° C. The resulting novel fibers were fluffed in a blender and characterized for their SRDF, LRDF, and other parameters. These materials have higher LRDF than the materials of Example 12. FIG. 15 shows the photographs of the materials of Example 13 at 7x. The results are as follows: dpf=33.3; SFBF=1.7; SRDF=46; LRDF=0.29; and L₀=5.4 mm; and L₁=3.8 mm.

Example 14

Example 14 discloses novel fibers having 4DG-shape fiber cross-section.

The 4DG-shaped fibers were extruded through the Egan extruder used in Example 1 using the spinnerette I-1004 whose apertures are illustrated in FIG. 16. The I-1004 spinnerette had 16 apertures. Following spinning parameters were used in this Example 14. PET having 0.70 IV and 0.2% TiO₂ was extruded. The extrusion temperature was 282° C. The quench air flow was 180 ft/min. The as-spun dpf was 19.9. The shape factor was equal to 3.9. The fibers were processed as in Example 1, heat shrunk in a dryer oven at 200° C. for 5 minutes, and cut into ¼" long materials. FIG. 17 shows the fiber cross-section of the as-spun fiber of Example 14. FIG. 18 shows the resulting novel fibers of Example 14. The structural properties of the Example 14 fibers are as follows: dpf=26; SFBF=1.7; SRDF=18; LRDF=0.10; L₀=7.3 mm; and L₁=6.6 mm.

Example 15

In Example 15, the ¼" cut fibers obtained from Example 14 were further shrunk in hot water at 90° C. for 1 minute and dried in an oven at 120° C. The resulting novel fibers were fluffed in a blender and characterized for their physical parameters. FIG. 19 shows the fiber cross-sections and FIG. 20 shows photographs of these novel fibers. The structural properties of the novel fibers of Example 15 are as follows: dpf=36; SFBF=1.9; SRDF=11; LRDF=0.35; L₀=4.4 mm; and L₁=2.9 mm.

Example 16

Example 16 discloses that addition of a surfactant to the SAP precursor solution enhances the initial rate of water absorption, R₁, in these novel fibers. Example 6 shows that R₁ for the novel fibers is 5.2 g/sec, significantly lower than that for the novel fibers of Example 1. Coating Camelot's precursor SAP solution on to the novel fibers of Example 1 reduces R₁. In this Example 16, LUROL 1852 was added to the SAP precursor solution prior to coating the base material of Example 1 with the SAP. LUROL 1852 is a nonionic, ethoxylated fatty acid ester obtained from Goulston Technology, Monroe, N.C. The LUROL 1852 composition is a trade secret. Ten grams of the novel fibers of Example 1 were coated with a 5% solution in water containing 1 gram of precursor solution SAP and 1 gram of LUROL 1852. The coated material was dried in an oven at 120° C. for 50 minutes and subsequently cured at 195° C. for 15 minutes. The resulting novel fibers were tested for absorbency behavior. The initial rate of water absorption, R₁, upon first insult was 15.2 g/sec. Thus, addition of appropriate surfactants to the SAP solution is one method of enhancing R₁ in the novel materials.

Example 17

Example 17 illustrates the utility of adding high levels of SAP powder to the novel fibers of the invention. This is

particularly desirable for thin diapers having high absorbent core density. Blends of the novel fibers of Example 1 (having 33 dpf and the H-cross-section) with superabsorbent polymer, Favor®, SXM70 from Stockhausen, which is a salt of crosslinked polyacrylic acid, were made in a laboratory blender at various blend levels as shown in Table 1. The above blended materials were tested for the absorbency behavior at 0.1118 g/cc density and the results are shown in Table 1.

TABLE 1

Absorbency Behavior of Blends Of TA and SAP at 0.1118 g/cc density						
S. No.	% SAP (by wt.)	Absorbency g. water/g. blend	Wet Collapse (%)	% Water Release at 1 Psi Load	R ₁ g/sec.	R _{avg} g/sec
1	20	10.3	-50	0.3	20.4	2.6
2	30	13.1	-70	0.6	20.6	2.8
3	40	13.1	-70	0.04	20.5	3.0
4	50	12.9	-64	1.3	21.6	2.5
5	60	15.3	-80	0.96	18.5	2.7
6	70	16.7	-94	0.83	18.5	2.6
7	0	8.6	-10	4.5	33.2	5.2

A negative number for wet collapse implies the structure actually "expanded" upon "wetting". Note the relatively low percentage of water release at 1 psi load.

Example 18

Example 18 discloses a process for making novel fibers by a spin-cut-shrink-lube process. In Example 18, fiber is spun at relatively high speeds of greater than 1500 m/min. High quench air velocity is used. This is a continuous process in which the fiber is cut to small staple lengths and in a continuous manner shrunk in hot (>80° C.) air and sprayed with hydrophilic lubricants. The resulting materials are highly convoluted, shrunk, short-cut materials.

Example 19

Example 19 illustrates novel fibers of the present invention made by the "spin-cut-shrink-lube" process. The extrusion system of Example 1 was used. The PET polymer was dried to a moisture level of less than or equal to 0.003 wt % in a Patterson Conaform dryer at 120° C. for a period of 8 hours. PET polymer having an IV 0.76 was extruded. The polymer was extruded at 283° C. through an Egan extruder using the spinnerette I-1042. The aperture design of the I-1042 spinnerette is shown in FIG. 5. The fibers were quenched with air at 120 ft/min. The take-up speed was 2500 m/min, as-spun dpf was 8.8. The shape factor of the fiber was 3.0. The as-spun fibers were cut into ½" long fibers and shrunk in hot water at 90° C. for 2 minutes. The resulting fibers were dried in an oven at 120° C. and fluffed in a laboratory blender. They were then sprayed with the lubricant of Example 10. The final lubricant on the fiber was about 0.8 wt % of the fibers. These fibers were allowed to air dry at room temperature (about 23° C.) for 16 hours. The physical characteristics of the resulting novel fibers were as follows: dpf=20.5; SFBF=1.5; SRDF=25; LRDF=0.20; L₀=6.4 mm; and L₁=5.1 mm.

The absorbency characteristics of the novel fibers at 0.0393 g/cc were as follows: Absorbency=14.2 g H₂O/g; Water release at 1 psi=32.5%; R₁ (g/sec)=20.8; and R_{avg}=1.9 g/sec.

Example 20

Example 20 discloses novel fibers having an Y-shaped cross-section. The Y-shaped product was made via a "spin-cut-shrink-lube" process using the following parameters.

PET having an IV 0.76 was extruded through the Egan extruder system described in Example 1, but using the spinnerette I-1195 having the Y shaped apertures shown in FIG. 21A. The polymer was extruded at 282° C. through the Egan extruder. The PET polymer was dried to a moisture level of less than or equal to 0.003 wt % in a Patterson Conaform dryer at 120° C. for a period of 8 hours. The quench air velocity was 185 ft/min. The take-up speed was 2200 m/min. The as-spun fiber was 65 dpf and a shape factor of 5.0. The as-spun fiber was cut ½" long and shrunk in hot water at 95° C. The cut, shrunk materials were dried in an oven at 120° C. The fiber was then lubricated with the lubricant of Example 10, at a level of 0.8-10% by weight. The novel fibers thus obtained were highly distorted and convoluted.

FIG. 22 shows a fiber cross-section of as-spun fibers of Example 20. FIG. 23 shows cross-sections of the novel fibers of Example 20. FIG. 24 is a photograph of novel fibers of Example 20 at 7×.

The measured physical properties of the novel fibers of Example 20 are as follows: dpf=132; SFBF=4.0; SRDF=36; LRDF=0.49; L₀=14.4 mm; and L₁=7.2 mm.

The absorbency characteristics of the novel fibers at 0.0393 g/cc were as follows: Absorbency=8.9 g H₂O/g; Wet Collapse (%)=8.3; Water released at 1 psi=22.8; R₁ (g/sec)=16.7; and R_{avg}=1.2 g/sec.

Example 21

Example 21 discloses the preparation of novel fibers having cross-sections as shown in FIG. 25. Example 12 used PET polymer of 0.76 I.V. with 0.2% TiO₂. The Egan extrusion system of Example 1 was used to extrude at 280° C. the polymer dried as in Example 1 through the spinnerette I-1198 having 11 orifices the design of which is shown in FIG. 26. The quench air velocity was 68 ft/min. The spinning lubricant was the same as in Example 19. The lubricant level of the fiber was about 0.8% by weight. The 25 dpf as-spun fibers were wound at 2500 m/min spinning speed on a Barmag SQ4SL winder. The as-spun fiber shape factor was 4.6. The as-spun fibers were cut into about ½" long fibers, shrunk in hot water at 90° C. for 1 minute and dried in oven at 120° C. The resulting materials were sprayed with the lubricant of Example 10 (0.8% by wt.) and dried overnight. FIG. 27 shows optical photographs of resulting materials at 7× and 40× magnification.

The physical characteristics of the novel fibers were characterized as follows: dpf=50.3; SFBF=3.1; SRDF=32; LRDF=0.23; L₀=8.7 mm; L₁=6.7 mm.

The absorbency characteristics of the novel fibers at 0.0393 g/cc were as follows: Absorbency=10.9 g H₂O/g material; Wet collapse=3.3%; Water released at 1 psi=28.2%; R₁=21.7 g/sec; and R_{avg}=1.9 g/sec

TEST PROCEDURES

Absorbent Property Parameters utilized in the present invention include the following:

- Absorbency, which is measured in grams of distilled water absorbed per gram of absorbent material.
- Wet collapse, which is the percentage decrease in the height of the absorbent material upon wetting.
- Water released, which is the percent of water that has been absorbed by the absorbent material that is released when the absorbent material is placed under a pressure of 1 pound per square inch (psi).
- R₁, which is the initial rate of water absorption upon a first wetting or insult of the absorbent material, and which is measured in grams of distilled water absorbed per second.

e. R_{avg} , which is the average initial rate upon the second through fifth contacts or insults of the absorbent material (i.e., $(R_2+R_3+R_4+R_5/4)$), and which has units of grams of distilled water absorbed per second.

The absorbent parameters were measured using a porous wire basket in which the absorbent materials are placed. The wire basket is made from a 0.008 inch diameter wire having a mesh size of 20. The wire basket has a cylindrical wall having a diameter of 6 centimeters. The height of the wall is 10 centimeters. The bottom of the basket is flat. The wire basket can be used to measure absorbent properties of any of the absorbent materials such as fluff pulp, synthetic absorbent materials, such as those disclosed hereinabove, SAP, and blends of the foregoing. The absorbent materials are prepared for deposition into the wire basket by first fluffing them in a laboratory blender. This step bulks up and uniformly mixes the absorbent material.

Next, a predetermined weight, W_1 grams of the fluffed absorbent material is deposited in the wire basket. The fluff absorbent material may then be pressed down so that it fills a specified volume of the wire basket in order to provide a specified and uniform density. Typically, 10 grams of the fluff absorbent material is deposited to the basket.

Next, the initial height of h_1 in centimeters of the absorbent material in the basket is measured, and the dry weight of the absorbent material and the basket is measured.

Next, 355 milliliters of distilled water is poured into a rectangular container having bottom dimensions of 20.6 centimeters by 23 centimeters. That base dimension and that volume of distilled water fills the container up 0.75 centimeters above the base. The height of the liquid above the base is the important factor in this step, because the height of the liquid above the base indicates how much of the basket will be submerged into distilled water in the following step.

Next, the basket is placed into the distilled water container for two seconds and then removed from the distilled water container. The basket is suspended for 10 seconds in order to allow the distilled water that this not retained by the absorbent material to drain out of the basket. Ten seconds after the basket has been removed from the liquid, the basket is weighed. The differences between the weight of the basket with the dry absorbent material and the weight of basket with the wet absorbent material W_2 is determined. R_1 is then determined. R_1 equals W_2 (in grams) divided by 2 (in seconds).

Ten minutes after the first insult, the process of placing the basket in the distilled water container for two seconds, suspending the basket for ten seconds, and then weighing the basket is repeated. The weight of the water picked up during the second insult (above the weight of water picked up during the first insult) W_3 is then recorded. The rate of water picked up during the second insult R_2 is then calculated. R_2 equals W_3 (in grams) divided 2 (in seconds).

The third insult occurs ten minutes after the second insult. The same procedures are followed to determine R_3 . Similarly, R_4 and R_5 are determined by repeating the steps for determining the weight of water pick up for a 2 second insult with the water at ten minute intervals.

The total water absorbency is determined by the following procedures.

Distilled water is placed into a distilled water container up to a height of about 15 centimeters. The basket containing the absorbent material is immersed in this distilled water container for ten seconds. The basket is slowly removed from the distilled water container in order to avoid any accelerative forces. Thus, the basket is removed from the

liquid over the period of between about 0.5 and 5 seconds. The basket is suspended so that it can drain for 30 seconds. After 30 seconds, the basket is weighed and the weight of the total water picked up is determined. The total water absorbency is then calculated as the grams of the water absorbed divided by the grams of the dry absorbent material.

Next, the (average) height of the absorbent material in the basket h_2 is measured. That is, if the absorbent material no longer has a uniform upper surface, an estimate is made of the average height of the upper surface. The wet collapse is then calculated based upon the initial height h_1 of the upper surface prior to wetting and the average height of the upper surface h_2 after wetting. The wet collapse is defined as a percentage change in the height as $[(h_1-h_2)/h_1]$ times 100.

The weight of water released (at 1 psi) is determined by the following procedure.

The basket with the absorbent material is submerged for ten seconds in distilled water using the same procedure for the determination of the total water absorbency discussed above. After suspending the basket out of the water for 30 seconds, a weight of 1991.5 grams is placed on top of the absorbent material in the basket for ten seconds. The 1991.5 grams load is a pressure of one pound per square inch. The 1991.5 gram weight is removed from the basket and the basket is weighed in order to determine the weight of the water absorbed after the one pound per square inch load had been applied. The percent water released due to the 1 psi pressure, is then calculated as 100 times the weight of the water released after the load had been applied divided by the weight of the absorbed water prior to when the load had been applied.

AS SPUN FIBER PARAMETERS

Shape Factor

The shape factor is the average of measurements on 20 cross-sections from a fiber. The shape factor is a measure of the deviation of the cross-section of the fiber from round. A round cross-section fiber has a shape factor of one. Irregularly shaped cross-sections have shape factors of greater than one. The mathematical upper limit of shape factors (which is not physically possible) is infinity. The shape factor is defined as the ratio of the perimeter, P_1 , of the fiber cross-section of the polymeric material to the hypothetical perimeter of, P_2 , of a round cross-section fiber having the same cross-sectional area, A , as the polymeric material. Therefore, the shape factor is defined as P_1 divided by the square root of $(4\pi A)$.

Specific Capillary Volume (SCV), Specific Capillary Surface Area (SCSA), Slenderness Ratio (SR), Capillary Channel Width

The following procedures are useful for determination of parameters used to define the as spun fibers and are taken verbatim from U.S. Pat. No. 5,200,248 at column 27 line 45 to column 30 line 12 and column 35 line 63 to column 35 line 59.

The procedures may require preparation of structures of varying lengths, some of which may exceed the length of the structure actually intended for use. It is to be understood that any structures shorter than lengths required by the procedures are evaluated on the basis of equivalent structures having the requisite lengths set forth in such procedures, except as may be otherwise specifically provided. Specific units may be suggested in connection with measurement and/or calculation of parameters described in the procedures. These units are provided for exemplary purposes only. Other units consistent with the intent and purpose of the procedures can be used.

The procedure used to determine Specific Capillary Surface Area (SCSA) and Specific Capillary Volume (SCV) of

a capillary channel structure is applied to a photomicrograph which shows a representative cross-section of the capillary channel structure. The cross-section of the structure is prepared for photomicrographing by embedding and microtoming techniques known to those skilled in the art. The following equations are used:

$$\text{SCSA} = \sum_{x=1}^i \text{of } P_x / \rho A_s, \quad (1)$$

$$\text{SCV} = \sum_{x=1}^i \text{of } A_{v_x} / \rho A_s, \quad (2)$$

wherein:

ρ = density of the solid (i.e., polymer);

A_s = area of the cross-section of capillary channel solid perpendicular to the capillary channel axis which bounds those capillary channels within the scope of criteria (a) and (b),

the sum over $x=1$ to i of P_x = the sum of the perimeters of the cross section of the solid forming each of the capillary channels, x , wherein each perimeter P_x bounds the capillary channel and is within the theoretical closure provided by C_x ;

the sum over $x=1$ to i of A_{v_x} = the sum of the void areas of the capillary channel structure wherein each A_{v_x} is calculated as the area bounded by the perimeter of the solid forming the channel and by C_x ; and

wherein i is the number of capillary channels in the structure, x refers to specific capillary channels of a capillary channel structure, and C_x corresponds to that part of a circle which is convex toward the interior of the channel and which is of a selected diameter that closes each capillary channel, x , wherein the circle, C_x is sized and positioned according to the following criteria:

- (a) the circle, C_x , is tangent to both walls of the capillary channel, x , at the points where it meets the walls; and
- (b) for each capillary channel, x , the circle C_x meeting
 - (a) maximizes A_{v_x} for each such channel, x , subject to the limitations that:
 - (i) the lines tangential to the intersection of C_x and the capillary channel walls intersect to form an angle of 120 degrees or less; and
 - (ii) C_x can have a radius of no greater than about 0.025 cm with respect to the actual scale of the capillary channel structure (circle radius will be enlarged by the same magnification factor applied to the actual structure in the photomicrograph).

For capillary channel structures having capillary channel wall fluid exchange orifices, the effect on SCV and SCSA will generally not be of numerical significance due to the thin walls of the capillary channel structures hereof, and can generally be disregarded in the calculations.

For capillary channels having multiple points of tangency with a circle of maximum radius, as provided above, the circle is positioned so as to maximize cross-sectional area (A_v) of the channel. For capillary channel structures having variation in cross-sectional size or shape, sufficient cross-sections can be evaluated to provide a representative weighted average SCV and or SCSA. If, however, any portion of the structure of linear length (in the axial direction of the capillary channels) of at least about 0.2 cm, preferably at least about 1.0 cm, has a SCV and SCSA within the claimed ranges hereof, that such structure is said to comprise a capillary channel structure of the present invention.

For capillary channel sheets, particularly those with capillary channel bases of relatively large width, a representa-

tive sample of the product having a fraction of the total width of the base can be substituted in place of the entire cross-section of the sheet. Such fractional sample of the sheet preferably has a width of at least about 0.5 cm. The purpose of SCV and SCSA, as defined above, is to provide quantitative analysis of structures characterized by open capillary channels. It is conceivable that such structures can have solid portions, appendages, and the like, which do not otherwise contribute to the definition of the capillary channels in this procedure. The above criteria will exclude perimeter and void areas corresponding to such nonfunctional portions of the structure from the calculations. Also, the cross-sectional area of nonfunctional solid elements is not to be included in the calculation of A_s . Exclusion of such perimeters and cross-sectional area is exemplified in more detail below.

FIG. 34 exemplifies a capillary channel structure fragment 800 and application of the SCV and SCSA procedure thereto. Shown is the fragment 800 of solid (i.e., polymer) having area A_s , capillary channel void areas A_{v_1} , A_{v_2} , A_{v_3} , A_{v_4} , with corresponding capillary channel perimeters P_1 , P_2 , P_3 , P_4 and theoretical closure circles C_1 , C_2 , C_3 , and C_4 . Also shown are circles C_5 , C_6 , C_7 . Radii r_1 , r_1'' , r_2 , r_2'' , r_3 , r_3'' , r_4 , r_4'' , r_5 , r_6 , r_7 are each perpendicular to the line tangent to the points of intersection m_1 , m_1'' , m_2 , m_2'' , m_3 , m_3'' , m_4 , m_4'' , m_5 , m_6 , m_7 , respectively, between the corresponding circles, C_1 , C_2 , C_3 , C_4 , C_5 , C_6 , C_7 and the solid material of fragment 800.

The circles C_1 , C_2 , C_3 , and C_4 are drawn so as to meet the above criteria. As can be seen circles C_1 and C_2 are limited in radius r_1 , r_2 by angles Y_1 , Y_2 which represent 120 degree angles of intersection between tangent lines t_1 , t_1'' , and between t_2 , t_2'' , respectively. A_{v_1} , A_{v_2} , A_{v_3} , and A_{v_4} are the areas bounded by perimeters P_1 , P_2 , P_3 , and P_4 and curves cc_1 , cc_2 , cc_3 , and cc_4 , respectively. Circles C_3 and C_4 represent the maximum size circle for capillary channel, wherein the angle of intersection of lines drawn tangent to the circle at points m_3 , m_3'' and at m_4 and m_4'' , respectively, would be less than 120 degrees. Thus, as represented in this exemplary figure, circles C_3 and C_4 would each have radius of 0.025 cm, after reduction for magnification effects. Perimeters are determined as the length of the solid boundary interior to the channels between the points of intersection between the circle and the solid for each channel. C_5 , C_6 , and C_7 represent circles of maximum radius applied to portions of the structure which do not qualify as capillary channels according to the criteria of this procedure. Hence, P and A_v for these circles would be zero. As perimeters P_1 , P_2 , P_3 , and P_4 , and curves cc_1 , cc_2 , cc_3 , and cc_4 , can be seen, the area of the solid between m_4 and m_4'' would be included within A_s since such solid corresponds to capillary channel walls bounding channels within the criteria for A_v in the calculation of SCV and SCSA. Areas A_{v_3} and $A_{v_3''}$, which are bounded by linear extensions of the radii r_3 , r_3'' , (said radii being perpendicular to the line of tangency between the circle C_3 and the walls of the channel), are not included in A_s . Likewise, radius r_4 truncates area A_{v_4} from the calculation A_s based upon extension of r_4 of circle C_4 .

Slenderness Ratio (S), Capillary Channel Width (CCW), and Average Structure Thickness (t_{ave}) are determined according to the procedures as follow. The procedures are implemented based upon a photomicrograph of a representative microtomed cross-section of the capillary channel structure, as previously described. For capillary channel structures having variation in Slenderness Ratio, Capillary Channel Width, and Average Structure Thickness in the axial direction of the capillary channels, sufficient cross-sections

should be evaluated to provide a representative weighted average Slenderness Ratio, Capillary Channel Width, and/or average structure thickness value. If, however, any portion of this structure of linear length in the axial direction of the capillary channels of at least about 0.2 cm, preferably at least about 1.0 cm, has a Slenderness Ratio, capillary channel width, and/or average structure thickness value within the ranges hereof, then such structure may comprise a capillary channel structure of the present invention. Reference is made to FIG. 35 for exemplary purposes of the procedures.

The following equations are used:

$$S=L^2/4A_{st}$$

$$t_{ave}=2A_{st}/L$$

wherein:

L=total solid perimeter of the cross-section of the structure; and

A_{st} =total area of the cross-section of the solid forming the structure perpendicular to the capillary channel axis.

The foregoing equation for Slenderness Ratio treats the fiber under consideration as if it has one channel-forming wall therein. For channeled fibers having a functional portion wherein one or more channels are present, the formula for Slenderness Ratio (S) can be given as:

$$S=L^2/4A_{st} N$$

wherein:

L and A_{st} are as hereinbefore defined; and

N=number of channel walls in the structure, said walls being those that have, on one or both sides, channels that are closable by straight closure chords.

CCW is the length of the straight closure chord of a capillary channel wherein said chord closes said intra-structure capillary channel and which tangentially contacts the points of intersection with the capillary channel walls of said channel in such a way to maximize the volume of the channel. (Portions of the structure which do not contribute open channels closable by straight closure chords should be disregarded prior to the above calculations.)

FIG. 35 shows, for exemplary purposes, a cross-section of a capillary channel structure 900 having chords W1, W2, W3, W4, W5, and W6 for capillary channels C1, C2, C3, C4, C5, and C6, respectively, thus N=6. FIG. 35 also indicates the region corresponding to total cross-sectional area A_{st} and indicates continuous line P_L , the length of which is the total perimeter L. X_a - X_f indicate points of tangency of the chords and the cross-section.

We claim:

1. A fluid management process comprising:

- (a) insulating a top sheet of an absorbent product with an aqueous fluid, the absorbent product being selected from the group consisting of a diaper, a catamenial, and an incontinent device;
- (b) acquiring of the aqueous fluid from the top sheet by an absorbent structure for temporarily acquiring and distributing a fluid wherein the absorbent structure comprises a plurality of fibers in proximity to each other and wherein the fibers are distorted, bulky synthetic polymeric fiber comprising: (a) a length of said fiber between 2 and about 37 millimeters, (b) a cross-section having a plurality of shapes varying along the length of said fiber, (c) a single fiber bulk factor between 0.5 and 10.0, (d) a short range distortion factor greater than 5, and (e) a long range distortion factor between 0.05 and 0.9; and

- (c) desorbing of the aqueous fluid from the absorbent structure to a storage core, the storage core being selected from the group consisting of fluff pulp; chemically modified fluff pulp; superabsorbent polymer; fiber having: (a) a length between 2 and about 37 millimeters, (b) a cross-section having a plurality of shapes varying along the length of said fiber, (c) a single fiber bulk factor between 0.5 and 10.0, (d) a short range distortion factor greater than 5, (e) a long range distortion factor between 0.05 and 0.9 and (f) a coating of a blend of superabsorbent polymer and surfactant; and combinations thereof.

2. A fluid management process comprising:

- (a) insulating a top sheet of an absorbent product with an aqueous fluid, the absorbent product being selected from the group consisting of a diaper, a catamenial, and an incontinent device;
- (b) acquiring of the aqueous fluid from the top sheet by an absorbent structure for temporarily acquiring and distributing a fluid wherein the absorbent structure comprises a plurality of fibers in proximity to each other and wherein the fibers are distorted, bulky synthetic polymeric fibers comprising: (a) a length of said fiber between 2 and about 37 millimeters, (b) a cross-section having a plurality of shapes varying along the length of said fiber, (c) a single fiber bulk factor between 0.5 and 10.0, (d) a short range distortion factor greater than 5, and (e) a long range distortion factor between 0.05 and 0.9;
- (c) desorbing of the aqueous fluid from the absorbent structure to a distribution layer; and
- (d) desorbing of the aqueous fluid from the distribution layer to a storage core being selected from the group consisting of fluff pulp; chemically modified fluff pulp; superabsorbent polymer; fiber having: (a) a length between 2 and about 37 millimeters, (b) a cross-section having a plurality of shapes varying along the length of said fiber, (c) a single fiber bulk factor between 0.5 and 10.0, (d) a short range distortion factor greater than 5, (e) a long range distortion factor between 0.05 and 0.9 and (f) a coating of a blend of superabsorbent polymer and surfactant; and combinations thereof.

3. The fluid management process of claim 2, wherein the distribution layer is selected from the group consisting of:

- (a) fibers having a Specific Capillary Volume of at least 2.0 cc/g and a Specific Capillary Surface Area of at least 2000 cm²/g, or a Slenderness Ratio of at least 9 and at least 30 percent of intra-fiber channels with a capillary channel width of less than 300 microns and
- (b) fibers having a Specific Capillary Volume of less than 2.0 cc/g or a Specific Capillary Surface Area of less than 2000 cm²/g, and a Slenderness Ratio of less than 9 or more than 70% of intra-fiber channels with a capillary channel width of greater than 300 microns.

4. The fluid management process of claim 3, wherein the fibers of (b) in claim 3 have a single fiber bulk factor of greater than 4.0.

5. A fluid management process comprising:

- (a) insulating a top sheet of an absorbent product with an aqueous fluid, the absorbent product being selected from the group consisting of a diaper, catamenial, and an incontinent device;
- (b) acquiring of the aqueous fluid from the top sheet by a distribution layer and an absorbent structure for temporarily acquiring and distributing a fluid wherein the absorbent structure comprises a plurality of fibers in

33

proximity to each other and wherein the fibers are distorted, bulky synthetic polymeric fibers comprising: (a) a length of said fiber between 2 and about 37 millimeters, (b) a cross-section having a plurality of shapes varying along the length of said fiber, (c) a single fiber bulk factor between 0.5 and 10.0, (d) a short range distortion factor greater than 5, and (e) a long range distortion factor between 0.05 and 0.9; and

(c) desorbing of the aqueous fluid from the distribution layer and the absorbent structure to a storage core, the storage core being selected from the group consisting of fluff pulp; chemically modified fluff pulp; superabsorbent polymer; fiber having: (a) a length between 2 and about 37 millimeters, (b) a cross-section having a plurality of shapes varying along the length of said fiber, (c) a single fiber bulk factor between 0.5 and 10.0, (d) a short range distortion factor greater than 5, (e) a long range distortion factor between 0.05 and 0.9 and

34

(f) a coating of a blend of superabsorbent polymer and surfactant; and combinations thereof.

6. The fluid management process of claim 5, wherein the distribution layer is selected from the group consisting of:

(a) fibers having a Specific Capillary Volume of at least 2.0 cc/g and a Specific Capillary Surface Area of at least 2000 cm²/g, or a Slenderness Ratio of at least 9 and at least 30 percent of intra-fiber channels with a capillary channel width of less than 300 microns and

(b) fibers having a Specific Capillary Volume of less than 2.0 cc/g or a Specific Capillary Surface Area of less than 2000 cm²/g, and a Slenderness Ratio of less than 9 or more than 70% of intra-fiber channels with a capillary channel width of greater than 300 microns.

7. The fluid management process of claim 6, wherein the fibers of (b) in claim 6 have a single fiber bulk factor of greater than 4.0.

* * * * *